Evaluation of Coral Reef Carbonate Production Models at a Global Scale

Nancy S. Jones[1], Andy Ridgwell[1], Erica J. Hendy[2,3]

[1] School of Geographical Sciences, University of Bristol, Bristol BS8 1SS, UK.

[2] School of Earth Sciences, University of Bristol, Bristol BS8 1RJ, UK.

[3] School of Biological Sciences, University of Bristol, Bristol BS8 1UG, UK.

Correspondence to: Erica J. Hendy (e.hendy@bristol.ac.uk)

Abstract

Calcification by coral reef communities is estimated to account for half of all carbonate produced in shallow water environments and more than 25% of the total carbonate buried in marine sediments globally. Production of calcium carbonate by coral reefs is therefore an important component of the global carbon cycle; it is also threatened by future global warming and other global change pressures. Numerical models of reefal carbonate production are needed for understanding how carbonate deposition responds to environmental conditions including atmospheric CO_2 concentrations in the past and into the future. However, before any projections can be made, the basic test is to establish model skill in recreating present day calcification rates. Here we evaluate four published model descriptions of reef carbonate production in terms of their predictive power, at both local and global scales. We also compile available global data on reef calcification to produce an independent observation-based dataset for the model evaluation of carbonate budget outputs. The four calcification models are based on functions sensitive to combinations of light availability, aragonite saturation (Ω_a) and temperature and were implemented within a specifically-developed global framework, the Global Reef Accretion Model (GRAM). No model was able to reproduce independent rate estimates of whole reef calcification, and the output from the temperature-only based approach was the only model to significantly correlate with coral-calcification rate observations. The absence of any predictive power for whole reef systems, even when consistent at the scale of individual corals, points to the overriding importance of coral cover estimates in the calculations. Our work highlights the need for an ecosystem modeling approach, accounting for population dynamics in terms of mortality and recruitment and hence calcifier abundance, in estimating global reef carbonate budgets. In addition, validation of reef carbonate budgets is severely hampered by limited and inconsistent methodology in reef-scale observations.

1 Introduction

Coral reefs are the product of long-term $CaCO_3$ accretion by calcifying organisms of the reef community (e.g. Hatcher, 1997; Perry et al., 2008), principally scleractinian corals and crustose coralline algae (CCA; e.g. Chave et al., 1972; Barnes and Chalker, 1990; Kleypas and Langdon, 2006; Mallela, 2007; Vroom, 2011). Coral reefs persist where net $CaCO_3$ accretion is achieved, i.e. where calcification by reef organisms exceeds dissolution and bioerosion (reviewed by Kleypas and Langdon, 2006; Fig. 1; Perry, 2011). Globally, coral reef calcification accounts for ~50% of shallow water (neritic) $CaCO_3$ production (Milliman, 1993) with an estimated budget of 0.65–0.83 Pg of $CaCO_3$ each year (Vecsei, 2004). Most of this annual global carbonate production (G_{global}) is preserved and buried, and so coral reefs play an important role in global carbon cycling (Vecsei, 2004) and hence the control of atmospheric CO_2.

Although the precise mechanisms by which calcification occurs in both corals and CCA are still poorly understood (reviewed by Allemand et al., 2011), it is thought that the rate of calcification is environmentally modulated by some combination of seawater aragonite saturation state (Ω_a), temperature (SST) and light availability (E) (Buddemeier and Kinzie, 1976; Kleypas and Langdon, 2006; Tambutté et al., 2011). As a result, it is anticipated that calcification on coral reefs is sensitive to climate change and ocean acidification (e.g. Kleypas et al., 1999; Erez et al., 2011; Hoegh-Guldberg, 2011). In particular the reduction of Ω_a due to ocean acidification (OA) causing decreased calcification of individual corals (reviewed by Kleypas and Yates, 2009; Andersson and Gledhill, 2013) and CCA (e.g. Anthony et al., 2008; Johnson and Carpenter, 2012; Johnson et al., 2014), and rising sea surface temperatures causing an increase in coral bleaching frequency due to heat stress (e.g. Donner et al., 2005; Baker et al., 2008; Frieler et al., 2013).

The global reef carbonate budget (i.e. G_{global}) is inherently difficult to evaluate because it is impossible to empirically measure this variable; instead it must be extrapolated from reef-scale observations. Vecsei (2004) synthesized census-based measurements to produce values of reef calcification rates (G_{reef}; Fig. 1) – that varied both regionally and with depth – to estimate G_{global} (0.65–0.83 Pg yr^{-1}). In contrast, the earlier estimate of G_{global} (0.9 Pg yr^{-1}) from Milliman (1993) is calculated from two modal values for G_{reef} (reefs: 0.4 g cm^{-2} yr^{-1}, lagoons: 0.08 g cm^{-2} yr^{-1}). Opdyke and

Walker (1992) found a lower estimate of reefal $CaCO_3$ budget of 1.4 Pg yr^{-1} derived from published Holocene $CaCO_3$ accumulation rates. Census-based methods calculate G_{reef} by summing the calcification by each reef-calcifier, multiplied by its fractional cover of the reef substrate (Chave et al., 1972; Perry et al., 2008). The calcification by individual components of the reef community may be derived from linear extension rates or published values for representative species (Vecsei, 2004). Often it is only calcification by scleractinian corals (G_{coral}) and coralline algae (G_{algae}) that are considered, due to their dominance in $CaCO_3$ production (e.g. Stearn et al., 1977; Eakin, 1996; Harney and Fletcher, 2003). G_{reef} values can also be calculated from the total alkalinity change (ΔTA) of seawater (e.g. Silverman et al., 2007; Shamberger et al., 2011; Albright et al., 2013) because precipitation of $CaCO_3$ decreases the total alkalinity (TA) of seawater whereas dissolution has the opposite effect (*sensu* Erez et al., 2011). By measuring the change in TA over a discrete time interval (Δt), it is possible to calculate the net ecosystem calcification (NEC) or net G_{reef} (Eq. 1; Albright et al., 2013):

$$G_{\mathrm{reef}} = -0.5 \cdot pz\frac{\Delta \mathrm{TA}}{\Delta t} \quad \text{(Eq. 1)}$$

where p is seawater density (kg m^{-3}) and z in water depth (m). G_{reef} measured using ΔTA accounts for inorganic precipitation (G_i; Fig.1) and dissolution; however, unlike census-based methods for calculating G_{reef}, it is not possible to break down the contribution of individual calcifers in the reef community (Perry, 2011). G_{coral} calculated from the width and density of annual bands within the colony skeleton is commonly used in census-based observations of G_{reef} (Fig. 1; Knutson et al., 1972).

Estimates of G_{global} alone tell us little about how reefs will be affected by climate change at a global scale. Instead, if coral calcification (G_{coral}) and reef community calcification rates (G_{reef}) can be numerically modeled as a function of the ambient physicochemical environment (e.g. E, Ω_a and SST), then the results could be scaled up to produce an estimate of G_{global} that could be re-calculated as global environmental conditions change. Examples of this approach (Table 1) include: (1) $\mathrm{ReefHab}^{\mathrm{Irr}}$, which is sensitive to E only and was initially developed to predict global reef calcification (G_{global}) and habitat area (Kleypas, 1997) and used to estimate changes in G_{global} since the last glacial maximum (LGM); (2) $\mathrm{Kleypas}^{\mathrm{Irr}\Omega}$, which simulates G_{reef} as a function of E and Ω_a and was originally developed to simulate carbonate chemistry changes in seawater on a reef transect (Kleypas et al., 2011); (3) Lough^{SST} which simulates G_{coral} as a function of SST and was derived from the strong relationship observed between SST and G_{coral} in massive *Porites* sp. colonies from the Great Barrier Reef (GBR), Arabian Gulf and Papua New Guinea (Lough, 2008); and (4) Silverman$^{SST\Omega}$, which simulates G_{reef} as a function of SST and Ω_a and was used to simulate the effects of projected future SSTs and Ω_a at known reef locations globally (Silverman et al., 2009). Although further models exist describing G_{coral} as a function of carbonate ion concentration ($[CO_3^{2-}]$; Suzuki et al., 1995; Nakamura and Nakamori, 2007) these are synonymous to the Ω_a function used in Kleypas$^{Irr\Omega}$ and Silverman$^{SST\Omega}$.

To date it remains to be demonstrated that any of the published models reproduce present day reef calcification rates (i.e. G_{reef}). Despite this, simulations of the effects of future climate scenarios have been attempted using calcification rate models. For example, McNeil et al. (2004) incorporated Lough^{SST} with the linear relationship observed between Ω_a and calcification in the BioSphere-2 project (Langdon et al., 2000), and predicted that G_{reef} will increase in the future. In contrast, a similar study by Silverman et al. (2009; Silverman$^{SST\Omega}$) concluded that coral reefs will start to dissolve. Whilst McNeil's study was criticized for its underlying assumptions (Kleypas et al., 2005), the contradictory predictions from these two models highlights the importance of comparing and fully evaluating reef calcification models, starting with their performance against present day observations.

Here we describe a novel model framework, the global reef accretion model (GRAM), and evaluate the four previously published calcification models (ReefHab^{Irr}, Kleypas$^{Irr\Omega}$, Lough^{SST} and Silverman$^{SST\Omega}$) in term of their skill in predicting G_{coral} and G_{reef}. The independent evaluation dataset comprises observations of G_{reef} from census-based methods and ΔTA experiments as well as G_{coral} measured from coral cores. The individual model estimates of G_{global} are discussed in comparison with previous empirical estimates. We highlight where model development is required in order to accurately simulate the effects of past and future environmental conditions on calcification rates in coral reefs.

2 Methods

2.1 Model Description

Four calcification models were selected for evaluation in global scale simulations: (1) ReefHab$^{\mathrm{Irr}}$ (Kleypas, 1997), (2) Kleypas$^{\mathrm{Irr}\Omega}$ (Kleypas et al., 2011), (3) Lough$^{\mathrm{SST}}$ (Lough, 2008) and (4) Silverman$^{\mathrm{SST}\Omega}$ (Silverman et al., 2009; Table 2). Previous applications for these models cover a hierarchy of spatial scales (colony, Lough$^{\mathrm{SST}}$; reef, Kleypas$^{\mathrm{Irr}\Omega}$ and global, ReefHab$^{\mathrm{Irr}}$ and Silverman$^{\mathrm{SST}\Omega}$) as well as representing different approaches for measuring G_{coral} (Fig. 1; Lough$^{\mathrm{SST}}$) and G_{reef} (Fig. 1; ReefHab$^{\mathrm{Irr}}$, Kleypas$^{\mathrm{Irr}\Omega}$ and Silverman$^{\mathrm{SST}\Omega}$). Any modification of the models from the published form is described below, and these are only made where necessary to fit them into the same GRAM framework.

2.1.1 ReefHab$^{\mathrm{Irr}}$

Kleypas (1997) developed ReefHab to predict changes in the global extent of reef habitat since the last Glacial Maximum (Kleypas, 1997). Like photosynthesis, calcification is light saturated (Allemand et al., 2011); as the rate of calcification increases toward a maximum value, it becomes light saturated after irradiance increases beyond a critical value. This curvilinear relationship can be described with various functions, however, hyperbolic-tangent and exponential functions have been found to best describe the relationship (Chalker, 1981). The ReefHab model calculates vertical accretion (G_{reef}) as a function of light penetration (E_z) and maximum growth rate (G_{max} = 1 cm yr^{-1}). The hyperbolic-tangent function uses a fixed light saturation constant (E_k = 250 µE m^{-2} s^{-1}) to generate a scaling factor for G_{max} (Eq. 2):

$$G_{\mathrm{reef}} = G_{\mathrm{max}} \cdot \tanh\left(\frac{E_z}{E_k}\right) \cdot TF \qquad E_z > E_c \qquad \text{(Eq. 2)}$$

where E_z is derived from the surface irradiance (E_{surf}) and the inverse exponent of the product of K_{490} and depth (z; Eq. 3). If E_z is less than the critical irradiance (E_c = 250 µE m^{-2} s^{-1}) G_{reef} = 0. TF is the topography factor (Eq. 4), which reduces G_{reef} in areas of low topographic relief.

$$E_z = E_{\mathrm{surf}} \cdot e^{-K_{490} z} \qquad \text{(Eq. 3)}$$

$$TF = \frac{ln(\alpha \cdot 100)}{5} \qquad \text{(Eq. 4)}$$

where α is calculated form a nine cell neighborhood (center index 2,2) by summing the inverse tangent of the difference between cell depths ($z_{i,j}$–$z_{2,2}$) divided by the distance between cell centers ($D_{i,j–2,2}$).

$$\alpha = \sum_{i=1}^{3} \sum_{j=1}^{3} \frac{\tan^{-1} z_{i,j} - z_{2,2}}{D_{\mathrm{i},j-2,2}} \qquad \text{(Eq. 5)}$$

Vertical accretion is converted to $CaCO_3$ mass by multiplying average carbonate density (2.89 g cm^{-3}) and porosity (50%) as defined by Kleypas (1997).

2.1.2 Kleypas$^{Irr\Omega}$

Anthony et al. (2011) performed laboratory flume incubations on *Acropora aspera* to parameterize the relationship between (day and night) calcification rates and Ω_a, determining the reaction order (n) and maximum calcification rates (k_{day} and k_{night}). The resultant model was then implemented by Kleypas et al. (2011), with the addition of an exponential light sensitive function that accounted for light enhanced calcification, to simulate seawater chemistry changes along a reef transect at Moorea, French Polynesia. The transect did not exceed 2 m in depth; therefore, it was appropriate to use the surface irradiance (E_{surf}) for the calculation of G_{reef}. In this study G_{reef} is calculated (Eq. 6) using E_z (Eq. 3) rather than E_{surf} because the maximum depth in the model domain is 100 m, greatly exceeding the depth of the original application.

$$G_{\mathrm{reef}} = \left(G_{\mathrm{max}}\left(1 - e^{-E_z/E_k}\right)^n + G_{\mathrm{dark}}\right) \cdot A_c \qquad \text{(Eq. 6)}$$

where A_c is the fractional cover of live coral (i.e. LCC 100%, A_c = 1). Here E_k is greater than in ReefHab^{Irr} (400 µE m^{-2} s^{-1} versus 250 µE m^{-2} s^{-1}) following the parameterization used by Kleypas et al. (2011). G_{reef} is calculated here in mmol m^{-2} d^{-1} and is divided into day and night rates (G_{max} and G_{dark}) both are calculated as a function of Ω_a. For this study it was necessary to introduce day length (L_{day}; hrs) to Eq. 7 and Eq. 8 because of the daily time step as opposed to the hourly timestep of the original model.

$$G_{max} = k_{day}(\Omega_a - 1)^n L_{day} \quad \text{(Eq. 7)}$$

$$G_{dark} = k_{dark}(\Omega_a - 1)^n (24 - L_{day}) \quad \text{(Eq. 8)}$$

L_{day} was calculated using the method described by Haxeltine and Prentice (1996), which uses Julian day (J_d) and latitude (*lat*) as follows:

$$L_{day} = 0 \qquad u \leq v \quad \text{(Eq. 9)}$$

$$L_{day} = 24 \cdot \frac{\cos^{-1} \cdot (-u/v)}{2\pi} \qquad u > -v, u < v \quad \text{(Eq. 10)}$$

$$L_{day} = 24 \qquad u \geq v \quad \text{(Eq. 11)}$$

where the variables *u* and *v* are calculated from *lat* and *aa* (a function of J_d; Eq. 14).

$$u = \sin(lat) \cdot \sin(aa) \quad \text{(Eq. 12)}$$

$$v = \cos(lat) \cdot \cos(aa) \quad \text{(Eq. 13)}$$

$$\text{aa} = -23.4^o \cdot \cos\left(\frac{360(J_d + 10)}{365}\right) \quad \text{(Eq. 14)}$$

$CaCO_3$ production in mmol was converted to mass, in grams, using the relative molecular weight of $CaCO_3$ ($MR = 100$).

2.1.3 Lough^{SST}

ReefHab^{Irr} and Kleypas$^{Irr\Omega}$ were both derived from theoretical understanding of the process of calcification and parameterized by values observed in the literature or *in situ*. In contrast, Lough^{SST} was derived from the observed relationship between annual calcification rates of massive *Porites* sp. colonies and local SST (Lough, 2008). A linear relationship (Eq. 15) was fitted to data from 49 reef sites from the Great Barrier Reef (GBR; Lough and Barnes, 2000), Arabian Gulf and Papua New Guinea (Lough, 2008), and accounted for 85% of the variance ($p < 0.001$).

$$G_{coral} = \frac{0.327 \cdot \text{SST} - 6.98}{365} \quad \text{(Eq. 15)}$$

2.1.4 Silverman$^{SST\Omega}$

Using ΔTA methods, Silverman et al. (2007) found a correlation between rates of inorganic precipitation (G_i) and net G_{reef}. Silverman et al. (2009) fitted observations to Eq. 16 to calculate G_i as a function of Ω_a and SST (Eq. 17):

$$G_{\mathrm{i}} = k_{\mathrm{SST}}(\Omega_a - 1)^{n_{\mathrm{SST}}} \qquad \text{(Eq. 16)}$$

$$G_{\mathrm{i}} = \frac{24}{1000}(-0.0177 \cdot \mathrm{SST}^2 + 1.4697 \cdot \mathrm{SST} + 14.893)(\Omega_a - 1)^{(0.0628 \cdot \mathrm{SST} + 0.0985)} \qquad \text{(Eq. 17)}$$

Incorporating Eq. 17 with SST and Ω_a sensitivity of coral calcification gives G_{reef} (Eq. 18):

$$G_{\mathrm{reef}} = k_r' \cdot \mathrm{G_i} \cdot e^{-(k_p'(\mathrm{SST} - T_{opt})/\Omega_a^2)^2} \cdot A_c \qquad \text{(Eq. 18)}$$

where $k_r^{'}$ (38 m^2 m^{-2}) and $k_p^{'}$ (1 $°C^{-1}$) are coefficients controlling the amplitude and width of the calcification curve. T_{opt} is the optimal temperature of calcification and is derived from the WOA 2009 monthly average SST (Locarnini et al., 2010) for June (in the Northern Hemisphere) and December (in the Southern Hemisphere).

2.1.5 Global Reef Accretion Model (GRAM) framework

The calcification production models above were implemented within our global reef accretion model (GRAM) framework. In this study, GRAM was implemented on a 0.25° x 0.25° global grid. Vertically, the model domain was resolved with 10 depth levels at equal 10m intervals with the fraction, by area, of a model cell (quasi-seabed) within each 10m layer recorded for calculating total carbonate production (Fig. 2). An environmental mask was imposed to limit $CaCO_3$ production to shallow-water tropical and sub-tropical areas. This mask was defined following Kleypas (1997; Kleypas *et al.*, 1999b): SST (>18°C), salinity (23.3-41.8 ‰) and depth (≤100m). Calcification was calculated on a daily basis over the course of one full calendar year and according to the environmental conditions at each grid cell (described below).

2.2 Input Data Description

Table 1 lists the data used to force GRAM. Ocean bathymetry was calculated from GEBCO One Minute dataset (https://www.bodc.ac.uk/data/online_delivery/gebco/) and mapped to the model grid. Monthly values for SST (Locarnini et al., 2010) and salinity (Antonov et al., 2010) were obtained from the World Ocean Atlas (WOA) 2009. These climatologies are reanalysis products of observations collected 1955-2009. The WOA data have a scaled vertical resolution with 24 layers, with a maximum depth of 1400 m; however, only surface values were used in this study. Daily photosynthetically available radiation (PAR), for the period 1991-1993, were obtained from the Bishop's High-resolution (DX) surface solar irradiance data (Lamont-Doherty Earth Observatory, 2000) derived from the International Satellite Cloud Climatology Project (ISCCP) data (Bishop and Rossow, 1991; Bishop et al., 1997). Monthly diffuse light attenuation coefficient of 490 nm light (K_{490}) was obtained from the Level-3 binned MODIS-Aqua products in the OceanColor database (available at http://oceancolor.gsfc.nasa.gov). Surface Ω_a was derived from the University of Victoria's Earth System Climate Model (Schmittner et al., 2009; Turley et al., 2010) for the decade 1990-2000. All input data were converted, without interpolating, to the same resolution as the model by recording the closest data point to the coordinates of the model grid cell's center. Missing values were extrapolated as an unweighted mean from the nearest values in the dataset found in the model cell's neighborhood (including diagonals) in an area up to 1° from the missing data point.

2.3 Evaluation dataset and methodology

An independent dataset of *in situ* measured calcification rates (G_{reef} and G_{coral}) was collated from the literature to evaluate model performance. In total, data from 11 coral core studies (Table 3; *Montastrea* and *Porites* sp.), 8 census-based and 12 ΔTA studies (Table 4) were assembled. This dataset is not comprehensive of all studies that have measured G_{reef} and G_{coral}; many older studies were excluded (e.g. Sadd, 1984) due to errors in calculation of G_{reef} that were resolved by Hubbard et al. (1990). The studies sampled cover a representative range of SST and Ω_a conditions in which present day reefs are found (Fig. 3). The positions of the *in situ* measurements were used to extract the equivalent data points from the gridded model output. Where location coordinates were not reported, Google Earth (available at http://earth.google.com) was used to establish the longitude and latitude, accurate to the model resolution of 0.25°. For uniformity, reported units of measurement were converted to g ($CaCO_3$) cm^{-2} yr^{-1}. The values of live coral cover (LCC) reported in the census-based and ΔTA studies were used to convert model G_{coral} to G_{reef}.

Model skill in reproducing the observed data was assessed using simple linear regression analysis preformed on observed calcification rates paired with their equivalent model value. When testing $Lough^{SST}$ against coral core data, values that were used in the original formulation of the model (Lough, 2008) were excluded so as to preserve the independence of the data. Similarly, when correlating $Silverman^{SST\Omega}$ with ΔTA data, the Silverman et al. (2007) datum was excluded. A global average LCC of 30% (Hodgson and Liebeler, 2002) was applied to model $CaCO_3$ production in model comparisons with census-based and ΔTA G_{reef} at a global scale. Global mean G_{reef} and G_{global} were calculated by applying a further 10% reefal area to model $CaCO_3$ production; this follows the assumption in Kleypas (1997) that 90% of the seabed is composed of unsuitable substrate for reef colonization and growth. Global and regional values are compared directly to the most recent estimates by Vecsei (2004), although other global estimates are also considered.

3 Results

3.1 Model carbonate production rates

Globally averaged values of G_{reef} (summarized in Table 5) vary little between ReefHab^{Irr} (0.65 ±0.35 g cm^{-2} yr^{-1}), Kleypas$^{Irr\Omega}$ (0.51 ±0.21 g cm^{-2} yr^{-1}) and Lough^{SST} (0.72 ±0.35 g cm^{-2} yr^{-1}), with Silverman$^{SST\Omega}$ producing a somewhat smaller value (0.21 ±0.11 g cm^{-2} yr^{-1}). A consistent feature across all models is the high carbonate production in the southern Red Sea along the coast of Saudi Arabia and Yemen and, in Kleypas$^{Irr\Omega}$ and Lough^{SST}, the East African coast (Fig. 4). In all models, there was very low carbonate production in the northern Red Sea compared to the south. There is higher carbonate production in the western Pacific than in the east, and along the Central American and northern South American coastline, and this is more pronounced in Kleypas$^{Irr\Omega}$ and Lough^{SST} than ReefHab^{Irr}. In scaling up to the global scale, estimates of G_{global} based on the models ReefHab^{Irr} (1.40 Pg yr^{-1}) and Silverman$^{SST\Omega}$ (1.1 Pg yr^{-1}) were substantially lower than for the other model setups (3.06 Pg yr^{-1} for Kleypas$^{Irr\Omega}$ and 4.32 Pg yr^{-1} for Lough^{SST}).

3.2 Observed carbonate production rates

Figure 5 shows the location and magnitude of the calcification observations. Coral core (G_{coral}) values are higher (0.5-2.8 g cm^{-2} yr^{-1}; full dataset in online supplementary material) than G_{reef} measurements from either census-based (0.1-0.9 g cm^{-2} yr^{-1}) or ΔTA (0.003-0.7 g cm^{-2} yr$^{-1;}$ Table 4) methods. In general, coral core data show decreasing G_{coral} with increasing latitude that is most pronounced in Hawaii and along both east and west Australian coastlines (Fig. 5). However, G_{coral} is not always smaller at higher latitudes, particularly in the Arabian Gulf (1.44 ±0.57 g cm^{-2} yr^{-1}; full dataset in online supplementary material) where it is toward the upper end of the observed range in G_{coral}. Despite its equitable latitude G_{coral} in the Gulf of Aqaba is twofold smaller (0.78 ±0.28 g cm^{-1} yr^{-1}). This result cannot be corroborated by ΔTA or census data as there is not observation for the Arabian Gulf, however, there is agreement that calcification in the Gulf of Aqaba is toward to lower end of the observed range for ΔTA measured G_{reef} (0.18 ±0.09 g cm^{-2} yr^{-1}) and G_{coral} measured from coral cores. In contrast, the census-based and ΔTA measurements show no latitudinal trends.

3.3 Model evaluation

Fig. 6 shows the correlation of corresponding model and observed calcification rates. With a slope of 0.97, the only significant correlation was that between Lough^{SST} and independent coral core data ($R^2 = 0.66$, $p < 0.0001$). The G_{reef} measured by Perry et al. (2013) in the Caribbean also fell close to a 1:1 line with Lough^{SST}, but the positive trend was not significant, either when considering just this data sub-set ($R^2 = 0.74$, $p = 0.14$, $n = 4$), or all ΔTA measured G_{reef} ($R^2 = 0.57$, $p = 0.14$, $n = 11$). The average regional G_{reef} estimated by all models showed little geographic difference (Fig. 7), which is in conflict with the conclusions of Vecsei (2004) who found the Atlantic, including Caribbean reefs, had the highest G_{reef} of all regions, followed by the Pacific and GBR (Table 5).

The Silverman$^{SST\Omega}$ model produced a global average G_{reef} (0.21 g cm^{-2} yr^{-1}) that falls within Vecsei's (2004) estimated range (0.09–0.27 g cm^{-2} yr^{-1}) but all other models were in excess of this (Table 5). Similarly, all model estimates of G_{global} (1.10–4.32 Pg yr^{-1}; Table 5) exceed estimates by Vecsei (2004; 0.65–0.83 Pg yr^{-1}). This difference was greatest for Kleypas$^{Irr\Omega}$ and Lough^{SST} (3.06 and 4.32 Pg yr^{-1} respectively). Global reef area (the area sum of all model cells where $G_{coral} > 0$ g cm^{-2} yr^{-1} and with the 10% reefal area applied) varies significantly between models (Table 5). ReefHab^{Irr} designates 195×10^3 km^2 as global reef area, which is less than that reported by Vecsei (2004; 304–345 x10^3 km^2), however, the other model setups estimate almost double this (500–592 x10^3 km^2).

4 Discussion

Four coral reef carbonate production models, contrasting in terms of dependent environmental controls, were evaluated at local, regional and global scales. The results show that only the model using SST alone ($\text{Lough}^{\text{SST}}$) is able to predict G_{coral}, and to a degree G_{reef}, with any statistical skill (Fig. 6). At the global scale, there is a large offset between the empirical and model estimates of G_{global} (Table 5), with the $\text{Lough}^{\text{SST}}$ G_{global} estimate approximately a factor of five greater than previous estimates by Milliman (1993) and Vecsei (2004). Although G_{global} values from $\text{ReefHab}^{\text{Irr}}$ and $\text{Silverman}^{\text{SST}\Omega}$ (1.4 Pg yr^{-1} and 1.1 Pg yr^{-1}) are significantly closer to the empirical estimates of G_{global} than the other models, their poor performance at the local reef scale (measured by G_{reef} and G_{coral}) undermines confidence in their predictive power at G_{global} scale. Since empirical estimates of G_{global} cannot themselves be evaluated, it is necessary to examine the factors involved in the estimation of G_{global}, and what role they play in terms of the disparity with the various model values.

Global reef area is used in extrapolating G_{reef} to G_{global} and so may have a significant effect on both model and empirical estimates of G_{global}. The $\text{Lough}^{\text{SST}}$ model achieves a global reef area of 567×10^3 km^2, comparable to the reef area used by Milliman (1993) and Opdyke and Walker (1992) of $617\text{x}10^3$ km^2 taken directly from Smith (1978). Whereas Vecsei (2004) used a revised reef area of $304–345\text{x}10^3$ km^2 (Spalding and Grenfell, 1997) which is almost half the size. Despite this difference in global reef area, Milliman (1993) and Vecsei (2004) estimate comparable values of G_{global}, further confounding evaluation of modeled G_{global}. The question of where to draw the line in terms of establishing reef boundaries is highly pertinent to modeling G_{global} as it dictates the area considered to be 'coral reef'. In our analysis, all grid cells with positive $CaCO_3$ production (i.e. $G > 0$ g cm^{-2} yr^{-1}) are considered to contain coral reef, even those that may be close to 0 g cm^{-2} yr^{-1}. Recently formed (immature) reefs with coral communities that have positive G_{reef} but where little or no $CaCO_3$ framework is present do exist (Spalding et al., 2001) and are accounted for by all four models. However, these coral communities are not included in reef area reported by Spalding and Grenfell (1997) and further information about their production rates and global abundance is needed to accurately quantify their significance in estimating G_{global} empirically. The presence of these coral communities has been correlated with marginal environmental conditions where low (highly variable) temperatures and high nutrient concentrations are seen (Couce et al., 2012). It logically follows that excluding these marginal reefs by tightening the physicochemical mask for SST to >20°C, as derived by Couce et al. (2012), would reduce global reef area and close the gap between empirical and model estimates of G_{global}. Further to this is the assumption within GRAM that the area between reef patches in a 'reef' cell (i.e. a cell with G > 0 g cm^{-2} yr^{-1}) accounts for 90% of the cell's area, with only 10% assumed to be composed of suitable substrate for reef formation and coral recruitment. The availability of suitable substrate has the greatest impact on the biogeography of coral reefs (Montaggioni, 2005) and so clearly needs to be evaluated to improve G_{global} estimates.

Reef area does not account for all of the disparity between estimates of G_{global}; attenuation of G_{reef} with depth may also be a causal factor. In both Atlantic and Indo-Pacific reefs, there was an exponential trend, decreasing with depth (≤60m), in G_{reef} data collated by Vecsei (2001). Modeled G_{reef} estimates should, therefore, also vary as a function of depth. In its published form, Lough$^{\text{SST}}$ produces the same value for G_{reef} throughout the water column; however, we can account for this model limitation by imposing a light-sensitive correction in the form of an exponential function to the output from Lough$^{\text{SST}}$ so that G_{reef} is a function of surface G_{reef} (G_{surf}) and depth (z; Eq. 19):

$$G_{\text{reef}} = G_{\text{surf}}.\, e^{-k_g z} \qquad \text{(Eq. 19)}$$

where k_g is a constant controlling the degree of attenuation with depth, in this estimate K_{490} was used. Equation 19 has the same form as that for calculating light availability (Eq. 3) used in both ReefHab$^{\text{Irr}}$ and Kleypas$^{\text{Irr}\Omega}$. Following this adjustment, the Lough$^{\text{SST}}$ G_{global} estimate is reduced to 2.56 Pg yr^{-1}, which is closer to empirical estimates. However, where light availability has been incorporated into other models no significant skill in predicting G_{coral} or G_{reef} was observed (ReefHab$^{\text{Irr}}$ and Kleypas$^{\text{Irr}\Omega}$ in Fig. 6).

A further factor that strongly affects G_{reef} and G_{global} estimates is the percentage of the reef covered by calcifying organisms (generally abridged as the term 'live coral cover', or LCC, although implicitly including other calcifiers). Applying the global average LCC of 30% clearly does not account for the large spatial and temporal variation in LCC (<1–43% in the dataset collated here; Table 4). Indeed, only a very limited number of Pacific islands (4/46) were found to have ≥30% LCC between 2000 and 2009 in the compilation of Vroom (2011). The global average of 30% was calculated from surveys of 1107 reefs between 1997 and 2001 (Hodgson and Liebeler, 2002) and represents total hard coral cover (LCC plus recently killed coral), so is an overestimate of LCC. Lough^{SST} has significant skill in replicating observed G_{coral} and has some skill in predicting G_{reef} values observed by a standardized census method (ReefBudget; Perry et al., 2012), but only when the local observed LCC is applied. If however, the global average LCC is applied to Lough^{SST} the correlation with G_{reef} is lost. In addition, the global average LCC may also account for the uniformity of regional G_{reef} values (Fig. 7), in contrast to the significant differences between regions identified by Vecsei (2004). For example, the Atlantic reefs (including the Caribbean) having the greatest G_{reef} (0.8 g cm^{-2} yr^{-1}) and reefs in the Indian Ocean the smallest G_{reef} (0.36g cm^{-2} yr^{-1}; Vecsei, 2004; Table 5). The pattern is reversed in terms of LCC, with Indo-Pacific reefs having ~35% hard coral cover compared to ~23% on Atlantic reefs (Hodgson and Liebeler, 2002). Further studies have shown that Caribbean reefs have greater G_{reef} and vertical accumulation rates than Indo-Pacific reefs, possibly due to increased competition for space on the later (Perry et al., 2008). These issues highlight the need for LCC to vary dynamically within models, allowing LCC to change spatially and temporally according to coral population demographics (mortality, growth and recruitment).

A specific example of unrealistic G_{reef} is seen for the Gulf of Carpentaria, where there are no known currently-accreting reefs (Harris et al., 2004) but projections of carbonate production according to output from the Lough^{SST} model are particularly high (Fig. 4). At least seven submerged reefs have been discovered in the Gulf of Carpentaria and a further 50 may exist, but these reefs ceased growth ~7 kyr BP when they were unable to keep-up with sea level rise (Harris et al., 2008). Failure to repopulate may be due to a combination of factors including very low larval connectivity in the Gulf of Carpentaria (Wood et al., 2014) and high turbidity, due to re-suspension of bottom sediments and particulate input from rivers (Harris et al., 2008). ReefHab^{Irr} is the only model to predict an absence of reef accretion in the majority of the Gulf of Carpentaria (Fig. 4) indicating that model sensitivity to light attenuation is essential. This example also raises two further points: firstly, that there are certainly undiscovered reefs that are not accounted for in empirical estimates of G_{global} and, secondly, that larval connectivity should be considered in simulations of G_{reef} because of its role in regulating LCC after disturbance (Almany et al., 2009; Jones et al., 2009).

In addition to static LCC, growth parameters (G_{max}, Eq. 2; E_k, Eq. 2 and 6; k_{day}, Eq. 7; k_{dark}, Eq. 8; k_r' and k_p', Eq. 18) did not vary geographically, having the same value in all model grid cells. This potentially affected the skill of Kleypas$^{Irr\Omega}$ in reproducing G_{coral} and G_{reef} since in the original application of the model (Kleypas et al., 2011) parameters (k_{day}, k_{dark} and E_k) were determined for observations at the location of the reef transect that was simulated. However, when looking at the correlation of model to data it is important to acknowledge the observational variability and error. The standard deviation, where reported, for census-based and ΔTA measured G_{reef} is ≤100% of the mean (Table 4). In addition to this variability, observational error is greater in census-based measurements of G_{reef} than ΔTA measurements (Vecsei, 2004). In a review of reef metabolism, G_{reef} was shown to vary considerably (0.05–1.26 g cm^{-2} yr^{-1}) depending on the LCC and CCA abundance (Gattuso et al., 1998). G_{reef} (measured by ΔTA) appears to vary little across Pacific coral reefs (Smith and Kinsey, 1976) but Gattuso et al. (1998) attribute this to the similarity of these reefs in terms of community structure and composition, as well as LCC. The apparent agreement between Lough^{SST} and Caribbean G_{reef} reported by Perry et al. (2013) indicates that a standardized experimental methodology for measuring G_{reef} is needed and implementing this would also provide a consistent dataset that would be invaluable for model evaluation. Unexpectedly, this result also suggests that Lough^{SST} may have skill in predicting G_{reef} in the Atlantic Ocean despite the absence of massive *Porites* sp. on which the Lough^{SST} model is built. *Porites* is a particularly resilient genera (e.g. Barnes et al., 1970; Coles and Jokiel, 1992; Loya et al., 2001; Hendy et al., 2003; Fabricius et al., 2011) and so applicability to other reef settings, coral genera and calcifiers as a whole is surprising. G_{coral} of a single species has been used in some census-based studies to calculate the G_{coral} of all scleractinian corals present

(Bates et al., 2010) and the Lough^{SST} results suggest this generalization may be appropriate.

Unlike census-based and ΔTA methodologies, G_{coral} measured from coral cores span multiple centuries (Lough and Barnes, 2000) and so smoothes the stochastic nature of coral growth and variations in reef accretion. G_{coral} and G_{reef} do vary a great deal temporally. For example, diurnal fluctuations may be up to five fold and result in net dissolution at night (e.g. Barnes, 1970; Chalker, 1976; Barnes and Crossland, 1980; Gladfelter, 1984; Constantz, 1986; McMahon et al., 2013). At intermediate time scales (weekly–monthly) G_{coral} may vary by a factor of three, with a degree of seasonal chronology (Crossland, 1984; Dar and Mohammed, 2009; Albright et al., 2013). Over longer time scales (≥1 yr), G_{coral} is less variable (Buddemeier and Kinzie, 1976) and both Hatcher (1997) and Perry et al. (2008) describe reef processes hierarchically according to temporal and spatial scales, finding that time spans of a year or more are required to study processes of reef accretion. The numerous observations of G_{coral} measured from coral cores is a further advantage over the sparse census and ΔTA determinations of G_{reef} which are generally more costly and labor-intensive. More observations of G_{reef} are, however, essential to improve statistical power and evaluation of model outputs. G_{reef} is also invaluable from a monitoring perspective (reviewed by Baker et al., 2008; e.g. Ateweberhan and McClanahan, 2010) by providing an effective measure of reef health that encompasses the whole reef community and accounting for different relative compositions of corals and algae (Vroom, 2011; Bruno et al., 2014). These benefits provide impetus for future measurements of G_{reef}, but our results demonstrate that a standardization of the methodology (as demonstrated in Perry et al., 2013) must be applied.

The four models used in this study all simplify the physiological mechanisms of calcification to predict G_{coral} and G_{reef} as a function of one or two external environmental variables. Calcification is principally a biologically controlled process in corals (e.g. Puverel et al., 2005); occurring at the interface between the polyp's aboral layer and the skeleton, which is separated from seawater by the coelenteron and oral layer (Gattuso et al., 1999). This compartmentalization means that the reagents for calcification (Ca^{2+} and inorganic carbon species) must be transported from the seawater through the tissue of the coral polyp to the site of calcification (reviewed in Allemand et al., 2011). Active transport of Ca^{2+}, bicarbonate ions (HCO_3^-) to the site of calcification and removal of protons (H^+) regulates the pH and Ω_a of the calcifying fluid (found between aboral ectoderm and skeleton) and requires energy (reviewed in Tambutté et al., 2011). Although the precise mechanism is unknown it is thought that in light zooxanthellate corals derive this energy from the photosynthetic products (principally oxygen and glycerol) of their symbionts, which is thought to partially explain the phenomenon of light enhanced calcification (LEC) (reviewed in Gattuso et al., 1999; Allemand et al., 2011; Tambutté et al., 2011). Both the ReefHab^{Irr} and Kleypas$^{Irr\Omega}$ models use this relationship with light to determine G_{coral}. However, corals that have lost their symbionts by 'bleaching' continue to show show enhanced calcification in the light (Colombo-Pallotta et al., 2010). As such, light intensity alone cannot account for changes in G_{coral}. Precipitation of aragonite from the calcifying fluid has been assumed to follow the same reaction kinetics as inorganic calcification with respect to Ω_a (Hohn and Merico, 2012), i.e. $k_p \cdot (\Omega - 1)^n$ (following Burton and Walter, 1987). Kleypas$^{Irr\Omega}$ and Silverman$^{SST\Omega}$ both use this function of seawater Ω_a in calculating calcification; however, despite the logical connection between Ω_a and G_{coral} neither model could reproduce observed G_{coral} values. Inorganic precipitation of aragonite increases linearly with temperature (Burton and Walter, 1987) as does respiration in corals when oxygen is not limited (Colombo-Pallotta et al., 2010). This temperature dependence may explain the strong correlation found by Lough (2008) between *Porites* growth and SST and the skill Lough^{SST} has shown in this study at reproducing G_{coral} observed values.

This study has shown that it is possible to predict global variations in coral carbonate production rates (G_{coral}) across an environmental gradient with significant skill simply as a function SST (Lough^{SST}). However, the Lough^{SST} model assumes a linear relationship between SST and coral calcification (G_{coral}) whereas at the extremes this is clearly not the case. For example, there is substantive evidence of declining coral calcification rates in recent decades coinciding with increasing temperatures (e.g. Cooper et al., 2008; De'ath et al., 2009; Cantin et al., 2010; Manzello, 2010; De'ath et al., 2013; Tanzil et al., 2013). Further laboratory experiments have found a Gaussian or bell-shaped response to increasing temperature with optima between 25 °C and 27 °C (e.g. Clausen and Roth, 1975; Jokiel and Coles, 1977; Reynaud-Vaganay et al., 1999; Marshall and Clode, 2004). In contrast to the linear SST-relationship in $Lough^{SST}$, Silverman et al. (2009; $Silverman^{SST\Omega}$) use the Gaussian relationship found by Marshall and Clode (2004) to modulate the rate of calcification derived from inorganic calcification (G_i) calculated from Ω_a. But, the output from $Silverman^{SST\Omega}$ is shown to be a poor predictor of G_{coral} or G_{reef} in this study. While using the $Lough^{SST}$ model alone is clearly not appropriate when applied to future temperature simulations, environmental gradients in G_{coral} established using $Lough^{SST}$ could be modulated to account for the physiological effect for heat-stress using degree-heating-months (e.g. Donner et al., 2005; McClanahan et al., 2007) or summer SST anomaly (e.g. McWilliams et al., 2005). This approach would then account for the evidence that corals exhibit widely differing temperature optima depending on their temperature history or climatological-average temperature (Clausen and Roth, 1975).

Since none of the models evaluated in this study showed significant skill in capturing global patterns of G_{reef}, none of the models provide a reliable estimate of G_{global}. Successful up-scaling of carbonate production to the reef (G_{reef}) and global domain (G_{global}) will require accounting for both depth attenuation (e.g. light sensitivity) and inclusion of population demographics affecting calcifier abundance. An ecosystem modeling approach that captures demographic processes such as morality and recruitment, together with growth, would result in a dynamically and spatially varying estimate of LCC. It is also clear that a standardized methodology for census-based measurements is required, as evident from the improved model–data fit in a subset of data collected using the ReefBudget methodology (Perry et al., 2012). Coral calcification rates have slowed by an estimated 30% in the last three decades (e.g. Bruno and Selig, 2007; Cantin et al., 2010; De'ath et al., 2013; Tanzil et al., 2013) reinforcing the pessimistic prognosis for reefs into the future under climate change (e.g. Hoegh-Guldberg et al., 2007; Couce et al., 2013; Frieler et al., 2013); numerical modeling is an essential tool for validating and quantifying the severity of these trends.

Acknowledgments

This work was supported by an AXA Research Fund Doctoral Fellowship to N.S.J., a Royal Society Advanced Fellowship and UK Ocean Acidification Research Program grant (NE/H017453/1) to A.R., and a RCUK Academic Fellowship to E.J.H. We would also like to thank Fiona Whitaker, Pru Foster, Sally Wood and Elena Couce for stimulating ideas and discussions and Jean-Pierre Gattuso (Editor) and reviewers (Bradley Opdyke and one anonymous) for their insightful comments.

References

Albright, R., Langdon, C., and Anthony, K. R. N.: Dynamics of seawater carbonate chemistry, production, and calcification of a coral reef flat, central Great Barrier Reef, Biogeosciences, 10, 6747-6758, 2013.

Allemand, D., Tambutté, É., Zoccola, D., and Tambutte, S.: Coral calcification, cells to reefs. In: Coral reefs: an ecosystem in transition, Dubinsky, Z. and Stambler, N., (Eds.), Springer, Dordrecht, Netherlands, 119-150, 2011.

Almany, G. R., Connolly, S. R., Heath, D. D., Hogan, J. D., Jones, G. P., McCook, L. J., Mills, M., Pressey, R. L., and Williamson, D. H.: Connectivity, biodiversity conservation and the design of marine reserve networks for coral reefs, Coral Reefs, 28, 339-351, 2009.

Andersson, A. J. and Gledhill, D.: Ocean acidification and coral reefs: effects on breakdown, dissolution, and net ecosystem calcification, Annu. Rev. Mar. Sci., 5, 321-348, 2013.

Anthony, K. R. N., Kleypas, J. A., and Gattuso, J.-P.: Coral reefs modify their seawater carbon chemistry - implications for impacts of ocean acidification, Global Change Biol., 17, 3655-3666, 2011.

Anthony, K. R. N., Kline, D. I., Diaz-Pulido, G., Dove, S., and Hoegh-Guldberg, O.: Ocean acidification causes bleaching and productivity loss in coral reef builders, P. Natl. Acad. Sci. USA, 105, 17442-17446, 2008.

Antonov, J. I., Seidov, D., Boyer, T. P., Locarnini, R. A., Mishonov, A. V., Garcia, H. E., Baranova, O. K., Zweng, M. M., and Johnson, D. R.: World Ocean Atlas 2009, volume 2: salinity. In: NOAA Atlas NESDIS 69, Levitus, S., (Ed.), U.S. Government Printing Office, Washington, D.C., 1-184, 2010.

Ateweberhan, M. and McClanahan, T. R.: Relationship between historical sea-surface temperature variability and climate change-induced coral mortality in the western Indian Ocean, Mar. Pollut. Bull., 60, 964-970, 2010.

Baker, A. C., Glynn, P. W., and Riegl, B.: Climate change and coral reef bleaching: an ecological assessment of long-term impacts, recovery trends and future outlook, Estuar. Coast. Shelf S., 80, 435-471, 2008.

Barnes, D. J.: Coral skeletons – an explanation of their growth and structure, Science, 170, 1305-1308, 1970.

Barnes, D. J. and Chalker, B. E.: Calcification and photosynthesis in reef-building corals and algae. In: Ecosystems of the World, 25: coral reefs, Dubinsky, Z., (Ed.), Elsevier Science Publishing Company, Amsterdam, The Netherlands, 109-131, 1990.

Barnes, D. J. and Crossland, C. J.: Diurnal and seasonal variation in the growth of staghorn coral measured by time-lapse photography, Limnol. Oceanogr., 25, 1113-1117, 1980.

Barnes, D. S., Brauer, R. W., and Jordan, M. R.: Locomotory response of *Acanthaster planci* to various species of coral, Nature, 228, 342-344, 1970.

Bates, N. R., Amat, A., and Andersson, A. J.: Feedbacks and responses of coral calcification on the Bermuda reef system to seasonal changes in biological processes and ocean acidification, Biogeosciences, 7, 2509-2530, 2010.

Bishop, J. K. B. and Rossow, W. B.: Spatial and temporal variability of global surface solar irradiance, J. Geophys. Res.-Oceans, 96, 16839-16858, 1991.

Bishop, J. K. B., Rossow, W. B., and Dutton, E. G.: Surface solar irradiance from the International Satellite Cloud Climatology Project 1983-1991, J. Geophys. Res.-Atmos., 102, 6883-6910, 1997.

Boucher, G., Clavier, J., Hily, C., and Gattuso, J.-P.: Contribution of soft-bottoms to the community metabolism (primary production and calcification) of a barrier reef flat (Moorea, French Polynesia), J. Exp. Mar. Biol. Ecol., 225, 269-283, 1998.

Bruno, J. and Selig, E.: Regional decline of coral cover in the Indo-Pacific: timing, extent, and subregional comparisons, PloS one, 2, e711, doi:710.1371/journal.pone.0000711, 2007.

Bruno, J. F., Precht, W. F., Vroom, P. S., and Aronson, R. B.: Coral reef baselines: how much macroalgae is natural?, Mar. Pollut. Bull., 80, 24-29, 2014.

Buddemeier, R. W. and Kinzie, R. A.: Coral growth, Oceanogr. Mar. Biol. Ann. Rev., 14, 183-225, 1976.

Burton, E. A. and Walter, L. M.: Relative precipitation rates of aragonite and Mg calcite from seawater: temperature or carbonate ion control?, Geology, 15, 111-114, 1987.

Cantin, N. E., Cohen, A. L., Karnauskas, K. B., Tarrant, A. M., and McCorkle, D. C.: Ocean warming slows coral growth in the central Red Sea, Science, 329, 322-325, 2010.

Carricart-Ganivet, J. P. and Merino, M.: Growth responses of the reef-building coral *Montastraea annularis* along a gradient of continental influence in the southern Gulf of Mexico, Bull. Mar. Sci., 68, 133-146, 2001.

Chalker, B. E.: Calcium-transport during skeletogenesis in hermatypic corals, Comp. Biochem. Phys. A, 54, 455-459, 1976.

Chalker, B. E.: Simulating light-saturation curves for photosynthesis and calcification by reef-building corals, Mar. Biol., 63, 135-141, 1981.

Chave, K. E., Smith, S. V., and Roy, K. J.: Carbonate production by coral reefs, Mar. Geol., 12, 123-140, 1972.

Chen, T., Yu, K., Shi, Q., Chen, T., and Wang, R.: Effect of global warming and thermal effluents on calcification of the *Porites* coral in Daya Bay, northern South China Sea, J. Trop. Oceanogr., 30, 1-9, 2011.

Clausen, C. D. and Roth, A. A.: Effect of temperature and temperature adaptation on calcification rate in the hermatypic coral *Pocillopora damicornis*, Mar. Biol., 33, 93-100, 1975.

Coles, S. L. and Jokiel, P. L.: Effects of salinity on coral reefs. In: Pollution in tropical aquatic systems, Connell, D. W. and Hawker, D. W., (Eds.), CRC Press, London, 147-166, 1992.

Colombo-Pallotta, M. F., Rodriguez-Roman, A., and Iglesias-Prieto, R.: Calcification in bleached and unbleached *Montastraea faveolata*: evaluating the role of oxygen and glycerol, Coral Reefs, 29, 899-907, 2010.

Constantz, B. R.: Coral skeleton construction a physiochemically dominated process, Palaios, 1, 152-157, 1986.

Cooper, T. F., De'ath, G., Fabricius, K. E., and Lough, J. M.: Declining coral calcification in massive *Porites* in two nearshore regions of the northern Great Barrier Reef, Global Change Biol., 14, 529-538, 2008.

Cooper, T. F., O'Leary, R. A., and Lough, J. M.: Growth of Western Australian corals in the Anthropocene, Science, 335, 593-596, 2012.

Couce, E., Ridgwell, A., and Hendy, E. J.: Environmental controls on the global distribution of shallow-water coral reefs, J. Biogeogr., 39, 1508-1523, 2012.

Couce, E., Ridgwell, A., and Hendy, E. J.: Future habitat suitability for coral reef ecosystems under global warming and ocean acidification, Global Change Biol., 19, 3592-3606, 2013.

Crossland, C. J.: Seasonal-variations in the rates of calcification and productivity in the coral *Acropora formosa* on a high-latitude reef, Mar. Ecol. Prog. Ser., 15, 135-140, 1984.

Dar, M. A. and Mohammed, T. A.: Seasonal variations in the skeletogensis process in some branching corals in the Red Sea, Thalassas, 25, 31-44, 2009.

De'ath, G., Fabricius, K., and Lough, J.: Yes - coral calcification rates have decreased in the last twenty-five years!, Mar. Geol., 346, 400-402, 2013.

De'ath, G., Lough, J. M., and Fabricius, K. E.: Declining coral calcification on the Great Barrier Reef, Science, 323, 116-119, 2009.

Donner, S. D., Skirving, W. J., Little, C. M., Oppenheimer, M., and Hoegh-Guldberg, O.: Global assessment of coral bleaching and required rates of adaptation under climate change, Global Change Biol., 11, 2251-2265, 2005.

Eakin, C. M.: Where have all the carbonates gone? A model comparison of calcium carbonate budgets before and after the 1982-1983 El Niño at Uva Island in the eastern Pacific, Coral Reefs, 15, 109-119, 1996.

Edinger, E. N., Limmon, G. V., Jompa, J., Widjatmoko, W., Heikoop, J. M., and Risk, M. J.: Normal coral growth rates on dying reefs: are coral growth rates good indicators of reef health?, Mar. Pollut. Bull., 40, 404-425, 2000.

Erez, J., Reynaud, S., Silverman, J., Schneider, K., and Allemand, D.: Coral calcification under ocean acidification and global change. In: Coral reefs: an ecosystem in transition, Dubinsky, Z. and Stambler, N., (Eds.), Springer, Dordrecht, Netherlands, 151-176, 2011.

Fabricius, K. E., Langdon, C., Uthicke, S., Humphrey, C., Noonan, S., De'ath, G., Okazaki, R., Muehllehner, N., Glas, M. S., and Lough, J. M.: Losers and winners in coral reefs acclimatized to elevated carbon dioxide concentrations, Nature Climate Change, 1, 165-169, 2011.

Frieler, K., Meinshausen, M., Golly, A., Mengel, M., Lebek, K., Donner, S. D., and Hoegh-Guldberg, O.: Limiting global warming to 2 °C is unlikely to save most coral reefs, Nature Climate Change, 3, 165-170, 2013.

Gattuso, J.-P., Allemand, D., and Frankignoulle, M.: Photosynthesis and calcification at cellular, organismal and community levels in coral reefs: a review on interactions and control by carbonate chemistry, Am. Zool., 39, 160-183, 1999.

Gattuso, J.-P., Frankignoulle, M., and Wollast, R.: Carbon and carbonate metabolism in coastal aquatic ecosystems, Annu. Rev. Ecol. Syst., 29, 405-434, 1998.

Gattuso, J.-P., Payri, C. E., Pichon, M., Delesalle, B., and Frankignoulle, M.: Primary production, calcification, and air-sea CO_2 fluxes of a macroalgal-dominated coral reef community (Moorea, French Polynesia), J. Phycol., 33, 729-738, 1997.

Gattuso, J.-P., Pichon, M., Delesalle, B., Canon, C., and Frankignoulle, M.: Carbon fluxes in coral reefs. I. Lagrangian measurement of community metabolism and resulting air-sea CO_2 disequilibrium, Mar. Ecol. Prog. Ser., 145, 109-121, 1996.

Gattuso, J.-P., Pichon, M., Delesalle, B., and Frankignoulle, M.: Community metabolism and air-sea CO_2 fluxes in a coral-reef ecosystem (Moorea, French Polynesia), Mar. Ecol. Prog. Ser., 96, 259-267, 1993.

Gladfelter, E. H.: Skeletal development in *Acropora cervicornis*: 3. a comparison of monthly rates of linear extension and calcium-carbonate accretion measured over a year, Coral Reefs, 3, 51-57, 1984.

Glynn, P. W., Wellington, G. M., and Birkeland, C.: Coral reef growth in the Galapagos: limitation by sea urchins, Science, 203, 47-49, 1979.

Grigg, R. W.: Darwin Point: a threshold for atoll formation, Coral Reefs, 1, 29-34, 1982.

Harney, J. N. and Fletcher, C. H.: A budget of carbonate framework and sediment production, Kailua Bay, Oahu, Hawaii, J. Sediment. Res., 73, 856-868, 2003.

Harris, P. T., Heap, A. D., Marshall, J. F., and McCulloch, M.: A new coral reef province in the Gulf of Carpentaria, Australia: colonisation, growth and submergence during the early Holocene, Mar. Geol., 251, 85-97, 2008.

Harris, P. T., Heap, A. D., Wassenberg, T., and Passlow, V.: Submerged coral reefs in the Gulf of Carpentaria, Australia, Mar. Geol., 207, 185-191, 2004.

Hart, D. E. and Kench, P. S.: Carbonate production of an emergent reef platform, Warraber Island, Torres Strait, Australia, Coral Reefs, 26, 53-68, 2007.

Hatcher, B. G.: Coral reef ecosystems: how much greater is the whole than the sum of the parts?, Coral Reefs, 16, S77-S91, 1997.

Haxeltine, A. and Prentice, I. C.: BIOME3: an equilibrium terrestrial biosphere model based on ecophysiological constraints, resource availability, and competition among plant functional types, Global Biogeochem. Cy., 10, 693-709, 1996.

Heiss, G. A.: Carbonate production by scleractinian corals at Aqaba, Gulf of Aqaba, Red Sea, Facies, 33, 19-34, 1995.

Hendy, E. J., Lough, J. M., and Gagan, M. K.: Historical mortality in massive *Porites* from the central Great Barrier Reef, Australia: evidence for past environmental stress?, Coral Reefs, 22, 207-215, 2003.

Hodgson, G. and Liebeler, J.: The global coral reef crisis: trends and solutions 1997-2001, Reef Check, California, USA, available at: http://reefcheck.org80 pp., 2002.

Hoegh-Guldberg, O.: Coral reef ecosystems and anthropogenic climate change, Reg. Environ. Change, 11, S215-S227, 2011.

Hoegh-Guldberg, O., Mumby, P. J., Hooten, A. J., Steneck, R. S., Greenfield, P., Gomez, E., Harvell, C. D., Sale, P. F., Edwards, A. J., Caldeira, K., Knowlton, N., Eakin, C. M., Iglesias-Prieto, R., Muthiga, N., Bradbury, R. H., Dubi, A., and Hatziolos, M. E.: Coral reefs under rapid climate change and ocean acidification, Science, 318, 1737-1742, 2007.

Hohn, S. and Merico, A.: Modelling coral polyp calcification in relation to ocean acidification, Biogeosciences, 9, 4441-4454, 2012.

Hubbard, D. K., Miller, A. I., and Scaturo, D.: Production and cycling of calcium carbonate in a shelf-edge reef system (St Croix, United States Virgin Islands): applications to the nature of reef systems in the fossil record, J. Sediment. Petrol., 60, 335-360, 1990.

Johnson, M. D. and Carpenter, R. C.: Ocean acidification and warming decrease calcification in the crustose coralline alga *Hydrolithon onkodes* and increase susceptibility to grazing, J. Exp. Mar. Biol. Ecol., 434, 94-101, 2012.

Johnson, M. D., Moriarty, V. W., and Carpenter, R. C.: Acclimatization of the crustose coralline alga *Porolithon onkodes* to variable pCO_2, Plos One, 9, e87678, doi:87610.81371/journal.pone.0087678, 2014.

Jokiel, P. L. and Coles, S. L.: Effects of temperature on the mortality and growth of Hawaiian reef corals, Mar. Biol., 43, 201-208, 1977.

Jones, G. P., Almany, G. R., Russ, G. R., Sale, P. F., Steneck, R. S., van Oppen, M. J. H., and Willis, B. L.: Larval retention and connectivity among populations of corals and reef fishes: history, advances and challenges, Coral Reefs, 28, 307-325, 2009.

Kayanne, H., Suzuki, A., and Saito, H.: Diurnal changes in the partial pressure of carbon dioxide in coral reef water, Science, 269, 214-216, 1995.

Kleypas, J. A.: Modeled estimates of global reef habitat and carbonate production since the last glacial maximum, Paleoceanography, 12, 533-545, 1997.

Kleypas, J. A., Anthony, K. R. N., and Gattuso, J.-P.: Coral reefs modify their seawater carbon chemistry - case study from a barrier reef (Moorea, French Polynesia), Global Change Biol., 17, 3667-3678, 2011.

Kleypas, J. A., Buddemeier, R. W., Archer, D., Gattuso, J.-P., Langdon, C., and Opdyke, B. N.: Geochemical consequences of increased atmospheric carbon dioxide on coral reefs, Science, 284, 118-120, 1999.

Kleypas, J. A., Buddemeier, R. W., Eakin, C. M., Gattuso, J.-P., Guinotte, J., Hoegh-Guldberg, O., Iglesias-Prieto, R., Jokiel, P. L., Langdon, C., Skirving, W., and Strong, A. E.: Comment on "Coral reef calcification and climate change: the effect of ocean warming", Geophys. Res. Lett., 32, L08601 , doi:08610.01029/02004gl022329, 2005.

Kleypas, J. A. and Langdon, C.: Coral reefs and changing seawater carbonate chemistry. In: Coral reefs and climate change: science and management, AGU, Washington, DC, 73-110, 2006.

Kleypas, J. A. and Yates, K. K.: Coral reefs and ocean acidification, Oceanography, 22, 108-117, 2009.

Knutson, D. W., Smith, S. V., and Buddemeier, R. W.: Coral chronometers: seasonal growth bands in reef corals, Science, 177, 270-272, 1972.

Lamont-Doherty Earth Observatory, C. U.: Bishop's high-resolution (DX) surface solar irradiance derived. Research data archive at the National Center for Atmospheric Research, Computational and Information Systems Laboratory, http://rda.ucar.edu/datasets/ds741.1/, 2000.

Land, L. S.: The fate of reef-derived sediment on the northern Jamaican island slope, Mar. Geol., 29, 55-71, 1979.

Langdon, C., Takahashi, T., Sweeney , C., Chipman, D., Goddard, J., Marubini, F., Aceves, H., Barnett, H., and Atkinson, M., J.: Effect of calcium carbonate saturation state on the calcification rate of an experimental coral reef, Global Biogeochem. Cy., 14, 639-654, 2000.

Lantz, C. A., Atkinson, M. J., Winn, C. W., and Kahng, S. E.: Dissolved inorganic carbon and total alkalinity of a Hawaiian fringing reef: chemical techniques for monitoring the effects of ocean acidification on coral reefs, Coral Reefs, 33, 105-115, 2014.

Locarnini, R. A., Mishonov, A. V., Antonov, J. I., Boyer, T. P., Garcia, H. E., Baranova, O. K., Zweng, M. M., and Johnson, D. R.: World Ocean Atlas 2009, volume 1: temperature. In: NOAA Atlas NESDIS 68, Levitus, S., (Ed.), U.S. Government Printing Office, Washington, D.C., 1-184, 2010.

Lough, J. M.: Coral calcification from skeletal records revisited, Mar. Ecol. Prog. Ser., 373, 257-264, 2008.

Lough, J. M. and Barnes, D. J.: Environmental controls on growth of the massive coral *Porites*, J. Exp. Mar. Biol. Ecol., 245, 225-243, 2000.

Loya, Y., Sakai, K., Yamazato, K., Nakano, Y., Sambali, H., and van Woesik, R.: Coral bleaching: the winners and the losers, Ecol. Lett., 4, 122-131, 2001.

Mallela, J.: Coral reef encruster communities and carbonate production in cryptic and exposed coral reef habitats along a gradient of terrestrial disturbance, Coral Reefs, 26, 775-785, 2007.

Manzello, D. P.: Coral growth with thermal stress and ocean acidification: lessons from the eastern tropical Pacific, Coral Reefs, 29, 749-758, 2010.

Marshall, A. T. and Clode, P.: Calcification rate and the effect of temperature in a zooxanthellate and an azooxanthellate scleractinian reef coral, Coral Reefs, 23, 218-224, 2004.

McClanahan, T. R., Ateweberhan, M., Muhando, C. A., Maina, J., and Mohammed, M. S.: Effects of climate and seawater temperature variation on coral bleaching and mortality, Ecol. Monogr., 77, 503-525, 2007.

McMahon, A., Santos, I. R., Cyronak, T., and Eyre, B. D.: Hysteresis between coral reef calcification and the seawater aragonite saturation state, Geophys. Res. Lett., 40, 4675-4679, 2013.

McNeil, B. I., Matear, R. J., and Barnes, D. J.: Coral reef calcification and climate change: the effect of ocean warming, Geophys. Res. Lett., 31, L22309, doi:22310.21029/22004GL021541, 2004.

McWilliams, J. P., Cote, I. M., Gill, J. A., Sutherland, W. J., and Watkinson, A. R.: Accelerating impacts of temperature-induced coral bleaching in the Caribbean, Ecology, 86, 2055-2060, 2005.

Milliman, J. D.: Production and accumulation of calcium carbonate in the ocean: budget of a non-steady state, Global Biogeochem. Cy., 7, 927-957, 1993.

Montaggioni, L. F.: History of Indo-Pacific coral reef systems since the last glaciation: development patterns and controlling factors, Earth-Sci. Rev., 71, 1-75, 2005.

Nakamori, T., Suzuki, A., and Iryu, Y.: Water circulation and carbon flux on Shiraho coral reef of the Ryukyu Islands, Japan, Cont. Shelf Res., 12, 951-970, 1992.

Nakamura, T. and Nakamori, T.: A geochemical model for coral reef formation, Coral Reefs, 26, 741-755, 2007.

Nakamura, T. and Nakamori, T.: Estimation of photosynthesis and calcification rates at a fringing reef by accounting for diurnal variations and the zonation of coral reef communities on reef flat and slope: a case study for the Shiraho reef, Ishigaki Island, southwest Japan, Coral Reefs, 28, 229-250, 2009.

Ohde, S. and van Woesik, R.: Carbon dioxide flux and metabolic processes of a coral reef, Okinawa, Bull. Mar. Sci., 65, 559-576, 1999.

Opdyke, B. N. and Walker, J. C. G.: Return of the coral reef hypothesis: basin to shelf partitioning of $CaCO_3$ and its effect in atmospheric CO_2, Geology, 20, 733-736, 1992.

Perry, C. T.: Carbonate budgets and reef framework accumulation. In: Encyclopedia of modern coral reefs: structure, form and process, Hopley, D., (Ed.), Springer, Netherlands, 185-190, 2011.

Perry, C. T., Edinger, E. N., Kench, P. S., Murphy, G. N., Smithers, S. G., Steneck, R. S., and Mumby, P. J.: Estimating rates of biologically driven coral reef framework production and erosion: a new census-based carbonate budget methodology and applications to the reefs of Bonaire, Coral Reefs, 31, 853-868, 2012.

Perry, C. T., Murphy, G. N., Kench, P. S., Smithers, S. G., Edinger, E. N., Steneck, R. S., and Mumby, P. J.: Caribbean-wide decline in carbonate production threatens coral reef growth, Nature Communications, 4, 1-8, doi:10.1038/ncomms2409, 2013.

Perry, C. T., Spencer, T., and Kench, P. S.: Carbonate budgets and reef production states: a geomorphic perspective on the ecological phase-shift concept, Coral Reefs, 27, 853-866, 2008.

Poulsen, A., Burns, K., Lough, J., Brinkman, D., and Delean, S.: Trace analysis of hydrocarbons in coral cores from Saudi Arabia, Org. Geochem., 37, 1913-1930, 2006.

Puverel, S., Tambutte, E., Zoccola, D., Domart-Coulon, I., Bouchot, A., Lotto, S., Allemand, D., and Tambutte, S.: Antibodies against the organic matrix in scleractinians: a new tool to study coral biomineralization, Coral Reefs, 24, 149-156, 2005.

Rayner, N. A., Parker, D. E., Horton, E. B., Folland, C. K., Alexander, L. V., Rowell, D. P., Kent, E. C., and Kaplan, A.: Global analyses of sea surface temperature, sea ice, and night marine air temperature since the late nineteenth century, J. Geophys. Res.-Atmos., 108, 4407, doi:4410.1029/2002JD002670, 2003.

Reynaud-Vaganay, S., Gattuso, J. P., Cuif, J. P., Jaubert, J., and Juillet-Leclerc, A.: A novel culture technique for scleractinian corals: application to investigate changes in skeletal $\delta 18O$ as a function of temperature, Mar. Ecol. Prog. Ser., 180, 121-130, 1999.

Sadd, J. L.: Sediment transport and $CaCO_3$ budget on a fringing-reef, Cane Bay, St Croix, United States Virgin Islands, Bull. Mar. Sci., 35, 221-238, 1984.

Schmittner, A., Oschlies, A., Matthews, H. D., and Galbraith, E. D.: Future changes in climate, ocean circulation, ecosystems, and biogeochemical cycling simulated for a business-as-usual CO_2 emission scenario until year 4000 AD, Global Biogeochem. Cy., 23, Gb3005, doi:3010.1029/2009GB003577, 2009.

Scoffin, T. P., Tudhope, A. W., Brown, B. E., Chansang, H., and Cheeney, R. F.: Patterns and possible environmental controls of skeletogenesis of *Porites lutea*, South Thailand, Coral Reefs, 11, 1-11, 1992.

Shamberger, K. E. F., Feely, R. A., Sabine, C. L., Atkinson, M. J., DeCarlo, E. H., Mackenzie, F. T., Drupp, P. S., and Butterfield, D. A.: Calcification and organic production on a Hawaiian coral reef, Mar. Chem., 127, 64-75, 2011.

Shi, Q., Yu, K. F., Chen, T. R., Zhang, H. L., Zhao, M. X., and Yan, H. Q.: Two centuries-long records of skeletal calcification in massive *Porites* colonies from Meiji Reef in the southern South China Sea and its responses to atmospheric CO_2 and seawater temperature, Science China-Earth Sciences, 55, 1-12, 2012.

Silverman, J., Lazar, B., Cao, L., Caldeira, K., and Erez, J.: Coral reefs may start dissolving when atmospheric CO_2 doubles, Geophys. Res. Lett., 36, L05606, doi:05610.01029/02008gl036282, 2009.

Silverman, J., Lazar, B., and Erez, J.: Effect of aragonite saturation, temperature, and nutrients on the community calcification rate of a coral reef, J. Geophys. Res.-Oceans, 112, C05004, doi:05010.01029/02006jc003770, 2007.

Smith, S. V.: Coral-reef area and the contributions of reefs to processes and resources of the world's oceans, Nature, 273, 225-226, 1978.

Smith, S. V. and Harrison, J. T.: Calcium carbonate production of the *mare incognitum*, the upper windward reef slope, at Enewetak Atoll, Science, 197, 556-559, 1977.

Smith, S. V. and Kinsey, D. W.: Calcium-carbonate production, coral-reef growth, and sea-level change, Science, 194, 937-939, 1976.

Smith, S. V. and Pesret, F.: Processes of carbon dioxide flux in the Fanning Island lagoon, Pac. Sci., 28, 225-245, 1974.

Spalding, M. D. and Grenfell, A. M.: New estimates of global and regional coral reef areas, Coral Reefs, 16, 225-230, 1997.

Spalding, M. D., Ravilious, C., and Green, E. P.: World atlas of coral reefs, Prepared at the UNEP World Conservation Monitoring Centre, University of California Press, Berkeley, USA, 424 pp., 2001.

Stearn, C. W., Scoffin, T. P., and Martindale, W.: Calcium-carbonate budget of a fringing reef on the West coast of Barbados: 1. zonation and productivity, Bull. Mar. Sci., 27, 479-510, 1977.

Suzuki, A., Nakamori, T., and Kayanne, H.: The mechanisms of production enhancement in coral-reef carbonate systems – model and empirical results, Sediment. Geol., 99, 259-280, 1995.

Tambutté, S., Holcomb, M., Ferrier-Pagès, C., Reynaud, S., Tambutté, É., Zoccola, D., and Allemand, D.: Coral biomineralization: from the gene to the environment, J. Exp. Mar. Biol. Ecol., 408, 58-78, 2011.

Tanzil, J. T., Brown, B. E., Dunne, R. P., Lee, J. N., Kaandorp, J. A., and Todd, P. A.: Regional decline in growth rates of massive *Porites* corals in Southeast Asia, Global Change Biol., 19, 3011-3023, 2013.

Turley, C., Eby, M., Ridgwell, A. J., Schmidt, D. N., Findlay, H. S., Brownlee, C., Riebesell, U., Fabry, V. J., Feely, R. A., and Gattuso, J.-P.: The societal challenge of ocean acidification, Mar. Pollut. Bull., 60, 787-792, 2010.

Vecsei, A.: Fore-reef carbonate production: development of a regional census-based method and first estimates, Palaeogeogr. Palaeocl., 175, 185-200, 2001.

Vecsei, A.: A new estimate of global reefal carbonate production including the fore-reefs, Global Planet. Change, 43, 1-18, 2004.

Vroom, P. S.: "Coral dominance": a dangerous ecosystem misnomer?, J. Mar. Biol., 2011, 164127, doi:164110.161155/162011/164127, 2011.

Weaver, A. J., Eby, M., Wiebe, E. C., Bitz, C. M., Duffy, P. B., Ewen, T. L., Fanning, A. F., Holland, M. M., MacFadyen, A., Matthews, H. D., Meissner, K. J., Saenko, O., Schmittner, A., Wang, H. X., and Yoshimori, M.: The UVic Earth system climate model: model description, climatology, and applications to past, present and future climates, Atmosphere-Ocean, 39, 361-428, 2001.

Wood, S., Paris, C. B., Ridgwell, A., and Hendy, E. J.: Modelling dispersal and connectivity of broadcast spawning corals at the global scale, Global Ecol. Biogeogr., 23, 1-11, 2014.

Tables

Table 1 Summary of calcification models implemented in the global reef accretion model (GRAM) framework.

Model	ReefHab^{Irr}	$\text{Kleypas}^{Irr\,\Omega}$	Lough^{SST}	$\text{Silverman}^{SST\,\Omega}$
Source	Kleypas (1997)	Kleypas et al. (2011)	Lough (2008)	Silverman et al. (2009)
Application or Formulation	Predicting changes to reef habitat extent, globally, since last glacial maximum.	Seawater carbonate chemistry changes on a transect in Moorea, French Polynesia†.	Derived from coral core (*Porites* sp.) measurements and temperature form the HadISST dataset (Rayner et al., 2003).	Future climate simulations at reef locations provided by ReefBase*.
Scale applied	Global	Reef	Colony	Reef/Global
E_{surf}	✓	✓	-	-
Ω_a	-	✓	-	✓
SST	-	-	✓	✓
Units	mm m^{-2} yr^{-1}	mmol m^{-2} hr^{-1}	g cm^{-2} yr^{-1}	mmol m^{-2} yr^{-1}

† Model output was compared to alkalinity changes measured *in situ* at Moorea by Gattuso et al. (1993), Gattuso et al. (1996), Gattuso et al. (1997); Boucher et al. (1998).

* ReefBase: A Global Information System for Coral Reefs (http://www.reefbase.org).

Table 2 Environmental data description (variable name, units, temporal and spatial resolution), and their sources, used to produce the physico-chemical domain mask (ranges shown) and force the calcification models (ReefHab^{Irr}, Kleypas$^{Irr\,\Omega}$, Lough^{SST} and Silverman$^{SST\,\Omega}$) in the global reef accretion model (GRAM) framework.

Variable	Unit	Temporal	Spatial	Mask Range	ReefHab^{Irr}	Kleypas$^{Irr\Omega}$	Lough^{SST}	Silverman$^{SST\Omega}$	Source
SST	°C	Monthly	1°	18.0 – 34.4	-	-	✓	✓	WOA 2009 (Locarnini et al., 2010) http://www.nodc.noaa.gov/OC5/WOA09/netcdf_data.html
Salinity	‰	Annual	1°	23.3 – 41.8	-	-	-	-	WOA 2009 (Antonov et al., 2010) http://www.nodc.noaa.gov/OC5/WOA09/netcdf_data.html
Bathymetry	m	—	$^1/_{60}$°	≤100	✓	✓	-	-	GEBCO One Minute Grid https://www.bodc.ac.uk/data/online_delivery/gebco/
PAR	dW m^{-2}	Daily	0.5°	—	✓	✓	-	-	Bishop's High-Resolution (DX) Surface Solar irradiance (Lamont-Doherty Earth Observatory, 2000) http://rda.ucar.edu/datasets/ds741.1/
k_{490}	m^{-1}	Annual	$^1/_{12}$°	—	✓	✓	-	-	OceanColor (2013) http://oceancolor.gsfc.nasa.gov/
Ω_a UVic	—	Decadal	3.6°×1.8°	—	-	✓	-	✓	University of Victoria's Earth System mate Model (Weaver et al., 2001; Schmittner et al., 2009; Turley et al., 2010)

SST – sea surface temperature; WOA – World Ocean Atlas; GEBCO – general bathymetric chart of the Oceans; BODC – British Oceanographic Data Centre; PAR – surface photosynthetically available radiation; k_{490} – 490nm light attenuation coefficient; Ω_a – aragonite saturation.

Table 3 Details of studies used for evaluating model calcification rates; observed coral calcification rates (G_{coral}) derived from annual density banding in coral cores; '—' indicates fields that were not reported. Full data, including values of G_{coral}, are supplied in online supplementary material. Studies are listed alphabetically by their ID.

ID	Source	Sea/Region	Genus	No. Sites	Period Observed	Latitude °N	Longitude °E
Ca	Carricart-Ganivet and Merino (2001)	Gulf of Mexico	Montastrea	6	1968 – 1991	19.08 to 22.53	264.15 to 270.35
Ch	Chen et al. (2011)	South China Sea	Porites	1	—	22.45	114.69
Co	Cooper et al. (2012)	Western Australia	Porites	6	1900 – 2010	-28.47 to -17.27	113.77 to 119.37
De	De'ath et al. (2009)	GBR	Porites	69	1900 – 2005	-23.55 to -9.58	142.17 to 152.75
Ed	Edinger et al. (2000)	Java Sea	Porites	5	1986 – 1996	-6.58 to -5.82	110.38 to 110.71
Fa	Fabricius et al. (2011)	Papua New Guinea	Porites	3	—	-9.83 to -9.74	150.82 to 150.88
Gr	Grigg (1982)	Hawaii	Porites	14	—	19.50 to 28.39	181.70 to 204.05
He	Heiss (1995)	Gulf of Aqaba	Porites	1	—	29.26	34.94
Po	Poulsen et al. (2006)	Arabian Gulf	Porites	4	1968 – 2002	27.20 to 28.35	48.90 to 49.96
Sc	Scoffin et al. (1992)	Thailand	Porites	11	1984 – 1986	7.61 to 8.67	97.65 to 98.78
Sh	Shi et al. (2012)	South China Sea	Porites	1	1710 – 2012	9.90	115.54

Table 4 Details of studies used for evaluating model calcification rates; observed calcification rates are for the reef community (G_{reef}) and are derived from census-based methods or alkalinity reduction experiments (ΔTA); '—' indicates fields that were not reported. Studies are listed alphabetically by their ID.

	ID	Source	Region	Genus or Groups	G_{reef} ±SD ($g\ cm^{-2}\ yr^{-1}$)	Cover ±SD (%) Coral	CCA	No. Sites	Period Observed	Latitude °N	Longitude °E
CENSUS-BASED	Ea	Eakin (1996)	Panama	Pocillopora & CCA	0.37 ±0.08	30 ±30	63 ±32†	—	1986 – 1995	7.82	278.24
	Gl	Glynn et al. (1979)	Galapagos	Pocillopora & CCA*	0.58	26-43		2	1975 – 1976	-1.22	269.56
	Hy	Harney and Fletcher (2003)	Hawaii	Porites, Montipora & CCA	0.12 ±0.04	32 ±27	44 ±29	60	—	21.41	202.27
	Ht	Hart and Kench (2007)	Torres Strait	Corals, CCA, Halimeda, foraminifera, molluscs	0.17 ±0.18	43	47	—	—	-10.21	142.82
	Hu	Hubbard et al. (1990)	St Croix	Montastrea, Agaricia, Porites & CCA*	0.12	16	59	4	—	17.78	295.19
	La	Land (1979)	Jamaica	Acropora, Montastrea, Agaricia & red/green algae*	0.52	30 ±16	—	—	—	18.55	282.60
	P1	Perry et al. (2013)	Bonaire	Montastrea, Agaricia, Diploria, Millepora & CCA	0.54 ±0.54	19 ±12	—	30	2010 – 2012	12.09	291.79
	P2		Belize		0.30 ±0.21	16 ±7	—	36		16.66	272.00
	P3		Grand Cayman		0.30 ±0.20	12 ±6	—	26		19.30	278.92
	P4		Bahamas		0.16 ±0.05	7 ±3	—	9		25.41	283.28
	St	Stearn et al. (1977)	Barbados	7 coral genera & CCA	0.90	37 ±22	41 ±14	6	1969-1974	13.20	300.36
ΔTA	Al	Albright et al. (2013)	GBR	NEC	0.48 ±0.48	9 ±2	8.5 ±3.5	1	Aug & Dec 2012	-18.33	147.65

G1	Gattuso et al. (1993)	French Polynesia	NEC	0.09	16[◊] (1-31)	—	2	Nov & Dec 1991	-17.48	210.00
G2	Gattuso et al. (1996)	French Polynesia	NEC	0.68	16[**]	4-21	2	July & Aug 1992	-17.48	210.00
		GBR	NEC	0.92	30	—	2	Dec 1993	-14.58	145.62
G3	Gattuso et al. (1997)	French Polynesia	NEC	0.003 ±0.002	~1	~3	1	Jul 1992	-17.48	210.00
Ka	Kayanne et al. (1995)	Japan	NEC	0.37	19[††]	<1[††]	1	Mar 1993 & 1994	24.37	124.25
La	Lantz et al. (2014)	Hawaii	NEC	0.60 ±0.15	14	5	2	Apr 2010 – May 2011	21.38	202.26
Na	Nakamura and Nakamori (2009)	Japan	NEC	0.16 ±0.27	20 ±19	—	10	Aug 2004, Jun–Aug 2006 & Jul/Aug 2007	24.37	124.25
Oh	Ohde and van Woesik (1999)	Japan	NEC	0.79	22	2	2	Oct 1993 – Oct 1995	26.17	127.50
Sh	Shamberger et al. (2011)	Hawaii	NEC	0.72 ±0.36	30	—	2	Jun 2008, Aug 2009 & Jan/Feb 2010	21.47	202.19
Si	Silverman et al. (2007)	Gulf of Aqaba	NEC	0.18 ±0.09	35[◊] (30-40)	—	4	2000 – 2002	29.51	34.92
Sm	Smith and Harrison (1977)	Marshall Islands	Acropora, Montipora & CCA	0.44 ±0.66	14 ±10	58 ±30	—	—	11.45	162.37
SP	Smith and Pesret (1974)	Line Islands	NEC	0.1	30	—	100	Jul/Aug 1972	4.00	201.00

CCA – crustose coralline algae; NEC – net ecosystem calcification.

[†] The value for CCA cover is the average of the % framework reported by Eakin (1996) that is defined as the area of dead coral upon which CCA grows.

[*]Authors note that the underlying assumptions for calculating calcification by algae may be unrealistic but make best use of the available data at the time of the study.

[◊] Median LCC values of the reported ranges were applied to model ouput for the regression analysis.

[**] The LCC range reported by Gattuso et al. (1993) was assumed to be the same as in the subsequent study at Moorea (Gattuso et al., 1996).

[††] Values reported in Suzuki et al. (1995) for study conducted in 1991 (Nakamori et al., 1992) at the same location.

Table 5 Average regional and global reef calcification rates (G_{reef}) and global $CaCO_3$ budgets (G_{global}) and reef areas derived from the four model setups (≤40m) and Vecsei (2004). Model G_{reef} is calculated as the total $CaCO_3$ production multiplied by global average live coral cover (LCC) of 30% (Hodgson and Liebeler, 2002) and 10% seabed reefal area with the exception of $ReefHab^{Irr}$, which uses a function of seabed topographic relief to modify total $CaCO_3$ production to give G_{reef}. Global reef area is 10% of the total area accounting for inter-reefal area.

	G_{reef} ±SD (≤40m; g cm^{-2} yr^{-1})				
Ocean Region	$ReefHab^{Irr}$	$Kleypas^{Irr\Omega}$	$Lough^{SST}$	$Silverman^{SST\Omega}$	Vecsei (2004)
Caribbean Sea	0.86 ±0.32	0.61 ±0.07	0.82 ±0.09	0.23 ±0.05	0.80 & 0.01*
North Atlantic Ocean	0.74 ±0.40	0.44 ±0.22	0.59 ±0.21	0.17 ±0.10	
South Atlantic Ocean	0.51 ±0.35	0.40 ±0.27	0.57 ±0.25	0.16 ±0.10	
Indian Ocean	0.65 ±0.36	0.54 ±0.17	0.82 ±0.17	0.22 ±0.08	0.36
North Pacific Ocean	0.67 ±0.35	0.49 ±0.22	0.70 ±0.22	0.20 ±0.11	0.65
South Pacific Ocean	0.67 ±0.30	0.61 ±0.20	0.93 ±0.21	0.29 ±0.12	
GBR	0.66 ±0.31	0.67 ±0.05	0.76 ±0.04	0.25 ±0.04	0.45
Global Metrics (≤40m)					
G_{global} (Pg yr^{-1})	1.40	3.06	4.32	1.10	0.65–0.83
Reef area (×10^3 km^2)	195	592	567	500	303–345
G_{reef} ±SD (g cm^{-2} yr^{-1})	0.65 ±0.35	0.51 ±0.21	0.72 ±0.35	0.21 ±0.11	0.09–0.27

*Values of G_{reef} for Atlantic/Caribbean framework and biodetrital reef respectively.

Figures

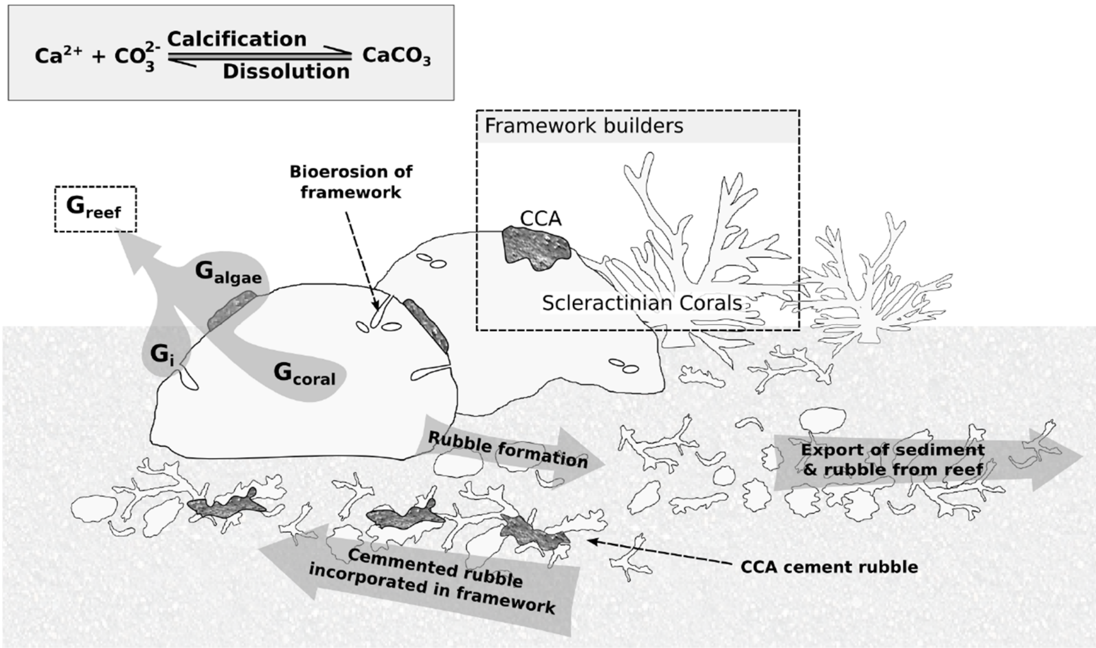

Fig. 1 Schematic illustrating the coral reef carbonate budget and the modeled parameters (G_{reef} and G_{coral}) used to quantify carbonate production. Carbonate framework is principally produced by scleractinian corals (G_{coral}) and crustose coralline algae (CCA; G_{algae}); the abiotic (inorganic) precipitation of carbonate cements (G_i) also occurs. Bioeroders breakdown the reef framework internally (e.g. worms, sponges) and externally (e.g. parrot fish, crown-of-thorns starfish). The rubble produced is incorporated back in to the framework, by cementation or burial, or exported from the reef. The observational data available to test models of carbonate budget include G_{coral} measured from coral cores, and G_{reef} calculated from a reef community census or the total alkalinity of surrounding seawater.

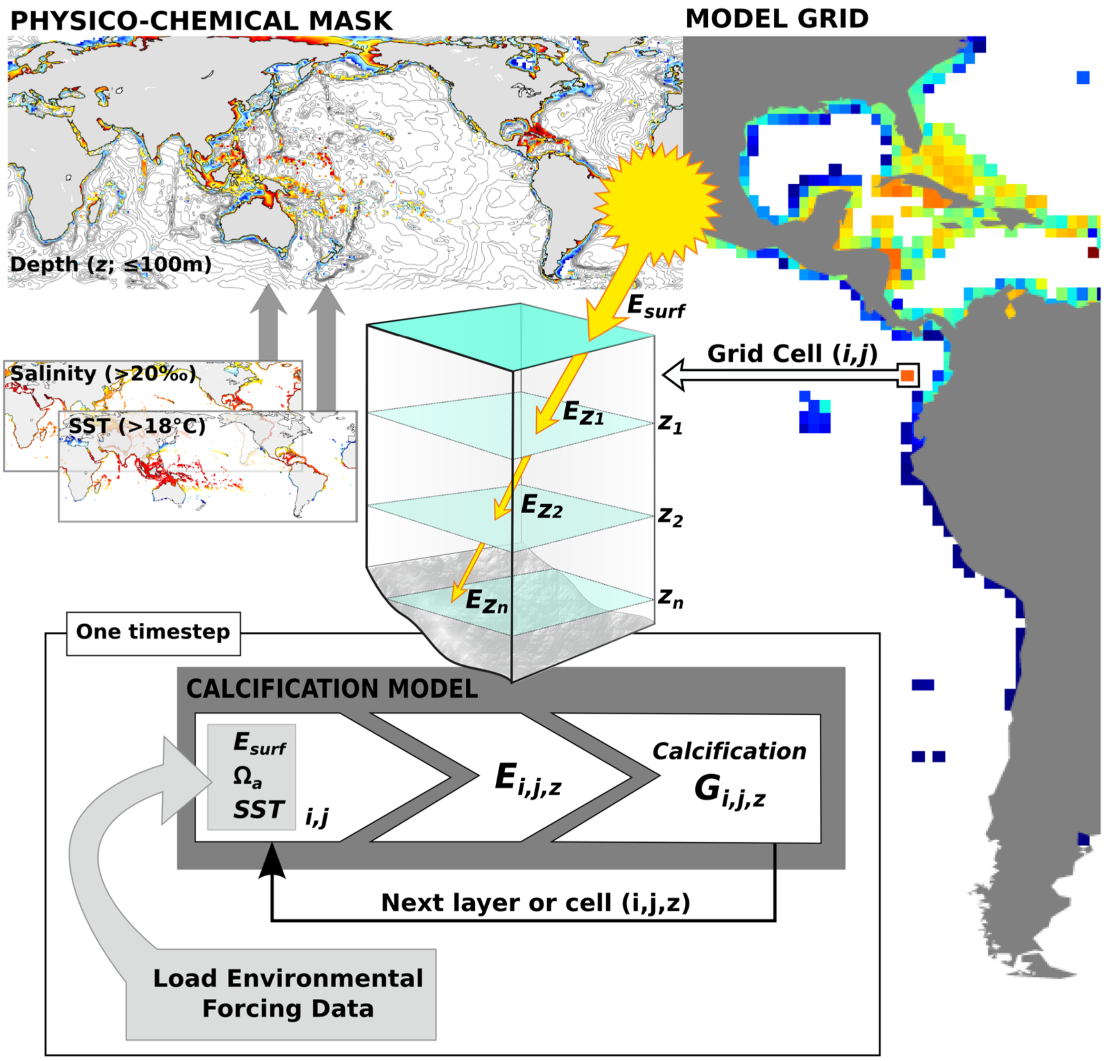

980
981 **Fig. 2** Schematic of logical steps at each timestep within GRAM. GRAM's domain is
982 defined by a bathymetric and physicochemical mask within which calcification is
983 calculated, at each timestep and in every domain grid cell, according to the
984 calculation model used. Where calcification is modeled as a function of light, the
985 availability of light at depth (E_z) is calculated for each model layer (z_i).

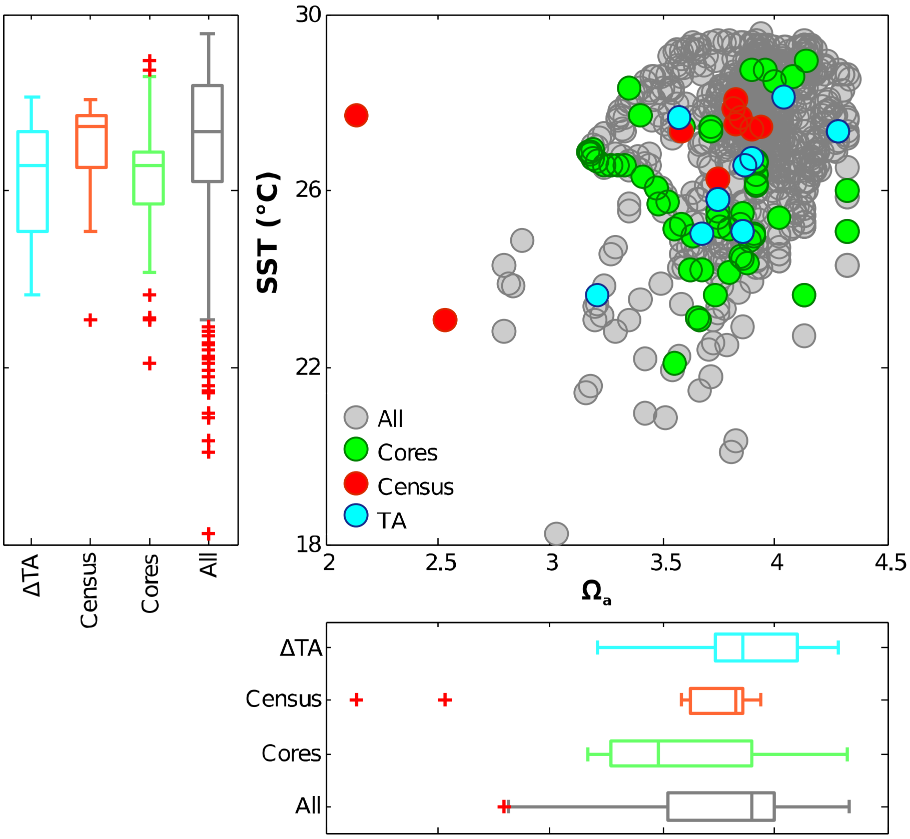

Fig. 3 Distribution of sea surface temperatures (SST) and aragonite saturation (Ω_a) at: (All) reef locations (ReefBase: A Global Information System for Coral Reefs. April, 2014. http://www.reefbase.org); (Cores) coral core data locations; (Census) census-based study and (ΔTA) ΔTA study locations. SST values are taken from WOA 2009 annual average values (Locarnini et al., 2010) and Ω_a values are derived from UVic model (Weaver et al., 2001; Schmittner et al., 2009; Turley et al., 2010) output. The range, 25th and 75th percentiles, median lines and outliers of SST and Ω_a are displayed in the box and whisker plots.

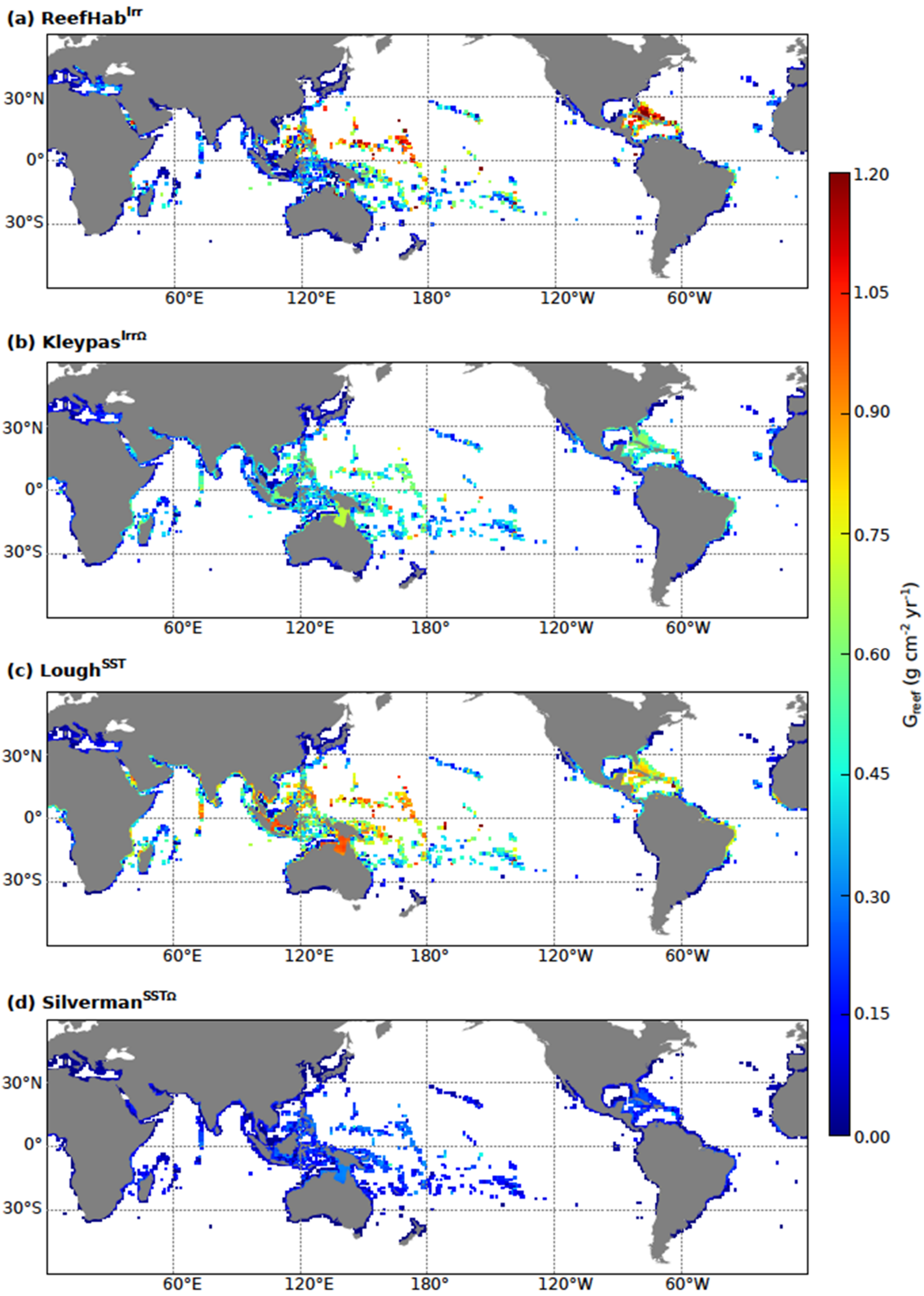

Fig. 4 Model outputs of reef carbonate production. Depth integrated (≤ 40 m) $CaCO_3$ production, with 30% live coral cover (LCC) and 10% seabed reefal area (G_{reef}) for: (a) ReefHab^{Irr}, (b) Kleypas$^{Irr\Omega}$, (c) Lough^{SST} and (d) Silverman$^{SST\Omega}$. G_{reef} values displayed are aggregated from the model resolution (0.25°) to a 1° grid to facilitate visualization.

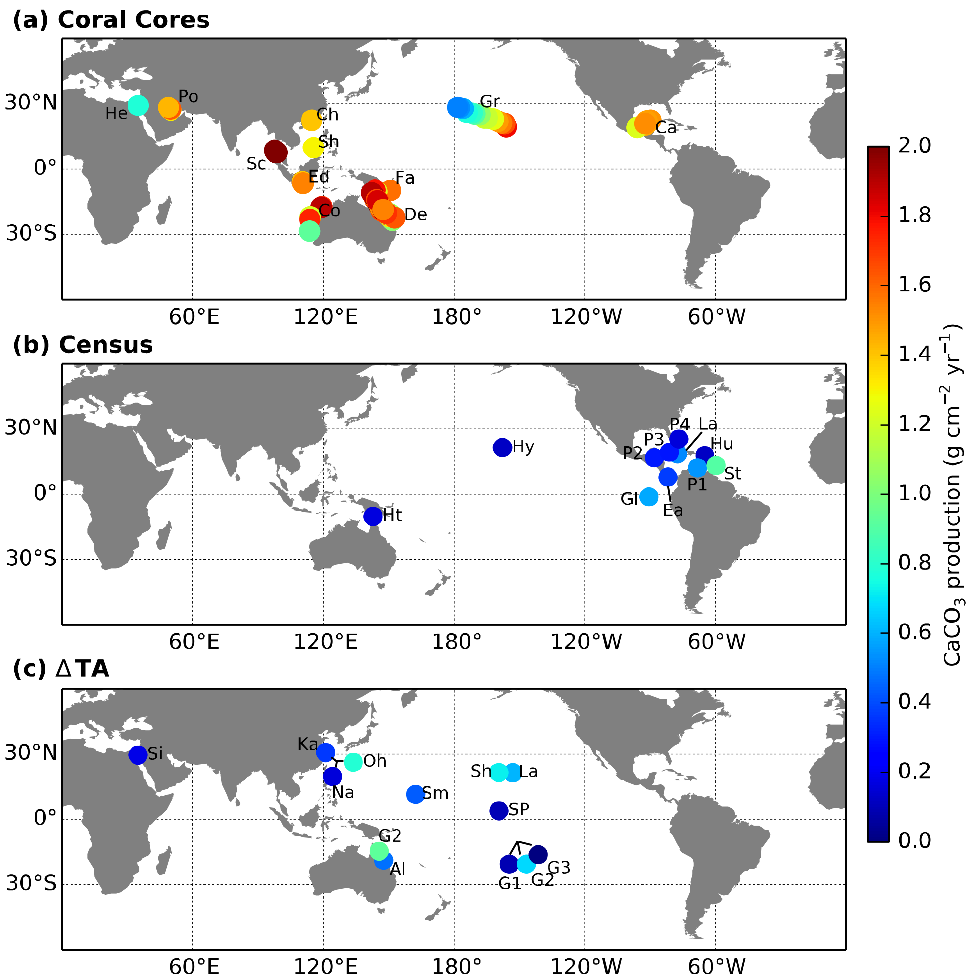

Fig. 5 Compilation of published reef carbonate production measurements. Location and magnitude of: (a) coral calcification (G_{coral}) observed in coral cores and, reef community calcification (G_{reef}) measured in (b) census-based and (c) ΔTA studies (See Tables 4 and 5 for study ID keys).

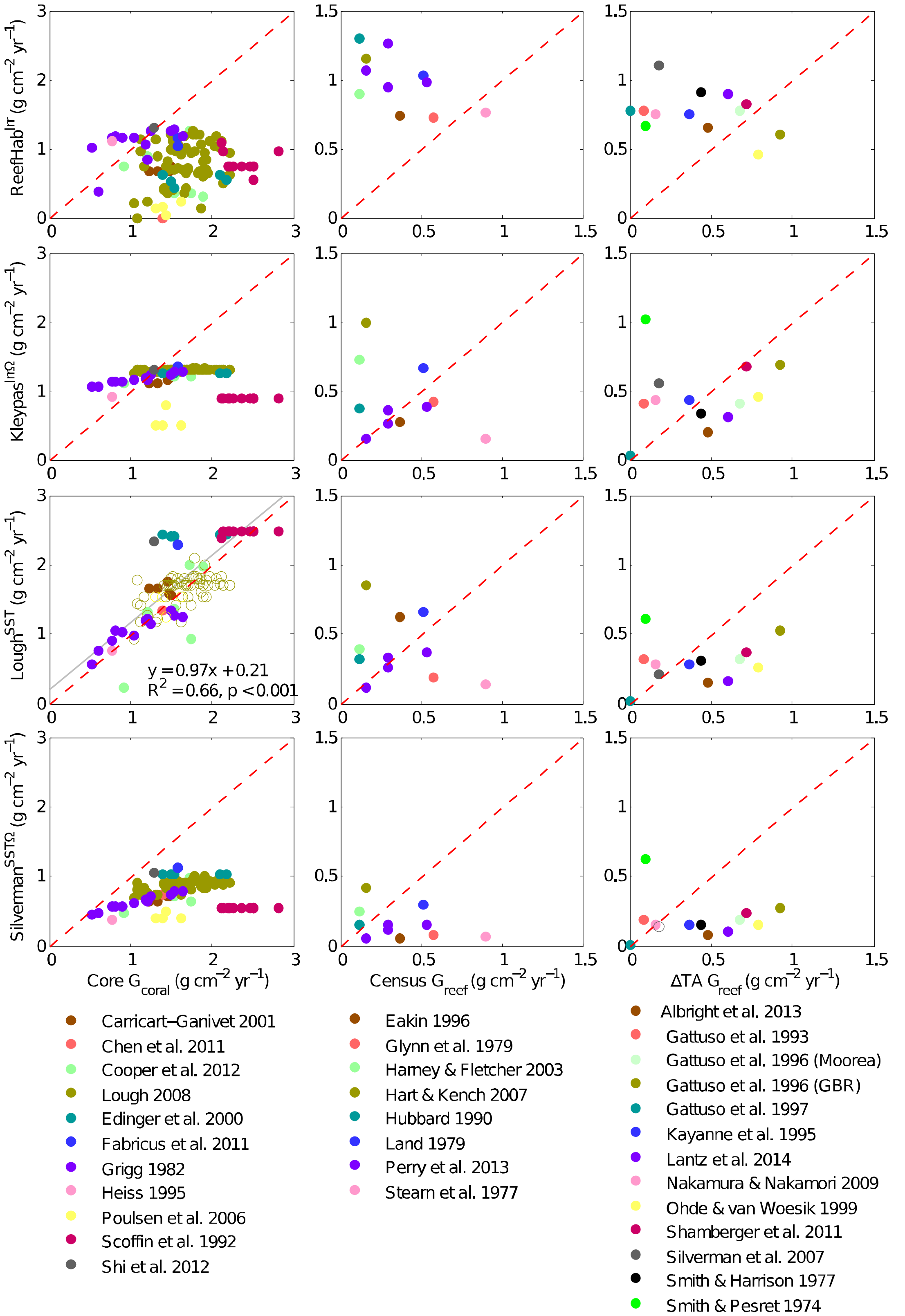

Fig. 6 Correlation of observed coral calcification (G_{coral}) and reef community calcification (G_{reef}) to model predictions (1:1 relationship shown as red dashed line). All model estimates are multiplied by the live coral cover (LCC) reported in the

observation studies to give G_{reef}, except ReefHab^{Irr} in which G_{reef} is calculated using a function of topographic relief (TF). The use of TF follows the method of Kleypas (1997); it was derived from empirical observation of reef growth and was a means to scale potential calcification (G_{coral}) to produce G_{reef} in the absence of global data for LCC. All significant linear regressions are plotted ($p < 0.05$; grey solid line) with equation and regression coefficient (R^2). Data used to develop a model are also plotted (open circles) but were excluded from the regression analysis to preserve data independence.

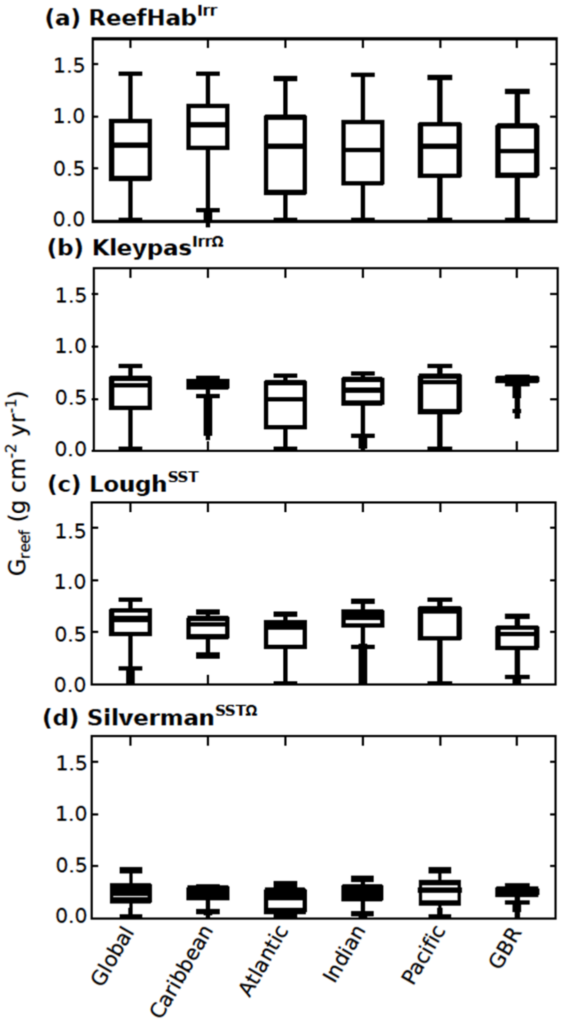

1018

1019 **Fig. 7** Box and whisker plots of model estimates for global and regional $CaCO_3$
1020 production. A live coral cover (LCC) of 30% is applied. Range (whiskers), 25th and
1021 75th percentiles (boxes), median (red line), and data outliers (+) are plotted.